Quasi-static strength and fatigue life of aerospace hole-to-hole bolted joints

Guillaume Pichon, Alain Daidié, Eric Paroissien, Audrey Benaben

Quasi-static strength and fatigue life of aerospace hole-to-hole bolted joints

Guillaume Pichon[1,2,*], Alain Daidié[1], Eric Paroissien[1], Audrey Benaben[2]

[1] *Institut Clément Ader (ICA), Université de Toulouse, ISAE-SUPAERO, INSA, IMT MINES ALBI, UT III, CNRS, 3 Rue Caroline Aigle, 31400 Toulouse, France*

[2] *Airbus Opérations S.A.S., 316 route de Bayonne 31300 Toulouse*

*To whom correspondence should be addressed:

Tel. +330688478724,

E-mail: gpichon@insa-toulouse.fr

Postal address: *3 Rue Caroline Aigle, 31400 Toulouse, France*

Abstract

Unlike hole coaxiality or other drilling defects, hole misalignment has never been a major concern in aeronautical structures as perfect bolt-hole alignment was ensured through the global assembly process. However, a new industrial philosophy called hole-to-hole, which aims to decrease industrial cost and time has bolt-hole misalignment as an unavoidable effect. A number of numerical studies have investigated the load distribution among fasteners of bolted composite joints in case of misalignments and has demonstrated significant impact on the static behaviour. Pylons are structural subcomponents joining the engines to the wings, that transmit high loads. Nevertheless, due to its dimensions, a pylon is a suitable structure for hole-to-hole assembly. This article presents the results of an experimental campaign on single-lap shear titanium bolted specimens with hole location errors. Several configurations of misalignment are examined and compared to a reference case with no defects. The static and fatigue strength results are studied for these different configurations. A comparative study of these results allows

the impact of misalignment on the mechanical strength to be estimated in relation to the reference case, without defects.

Keywords: experimental, clearance, misalignments, titanium, bolt preload, fatigue, pylon

1. Introduction

Although the aviation sector has been severely affected by the global health crisis linked to COVID-19 [1], the need for innovation is still strong in this challenging sector. Competitiveness has even been strengthened by the growing interest that states and the general public are showing in modern ecological challenges. The objective of global decarbonisation for the aeronautics industry has an impact on every organisation involved in this sector [2].

Above all, aircraft manufacturers must develop technology to ensure a sustainable transition. Composite materials are the backbone of developments intended to decrease the mass of structures and thus reduce fuel consumption. The second main interest for aircraft manufacturers is to become significant participants in industry 4.0, for better agility in both design and manufacturing. This transition is achievable by the re-engineering of processes.

For example in the context of aeronautical structures, digital metrology assisted assembly is a new way of integrating dimensional variation management at the manufacturing stage of large scale structures [3]. The present paper focuses on the "hole-to-hole" (H2H) bolted assembly process introduced by **Bloem [4]**, which offers a great opportunity to revolutionize aeronautic assembly lines by having structural parts individually drilled before the assembly phase. This process involves inherent misalignments of bolt holes when parts are mated, making bolt installation impossible, as illustrated in Figure 1. The solution proposed by **Bloem [4]** is to slightly increase bolt hole diameters so that assembly is still feasible.
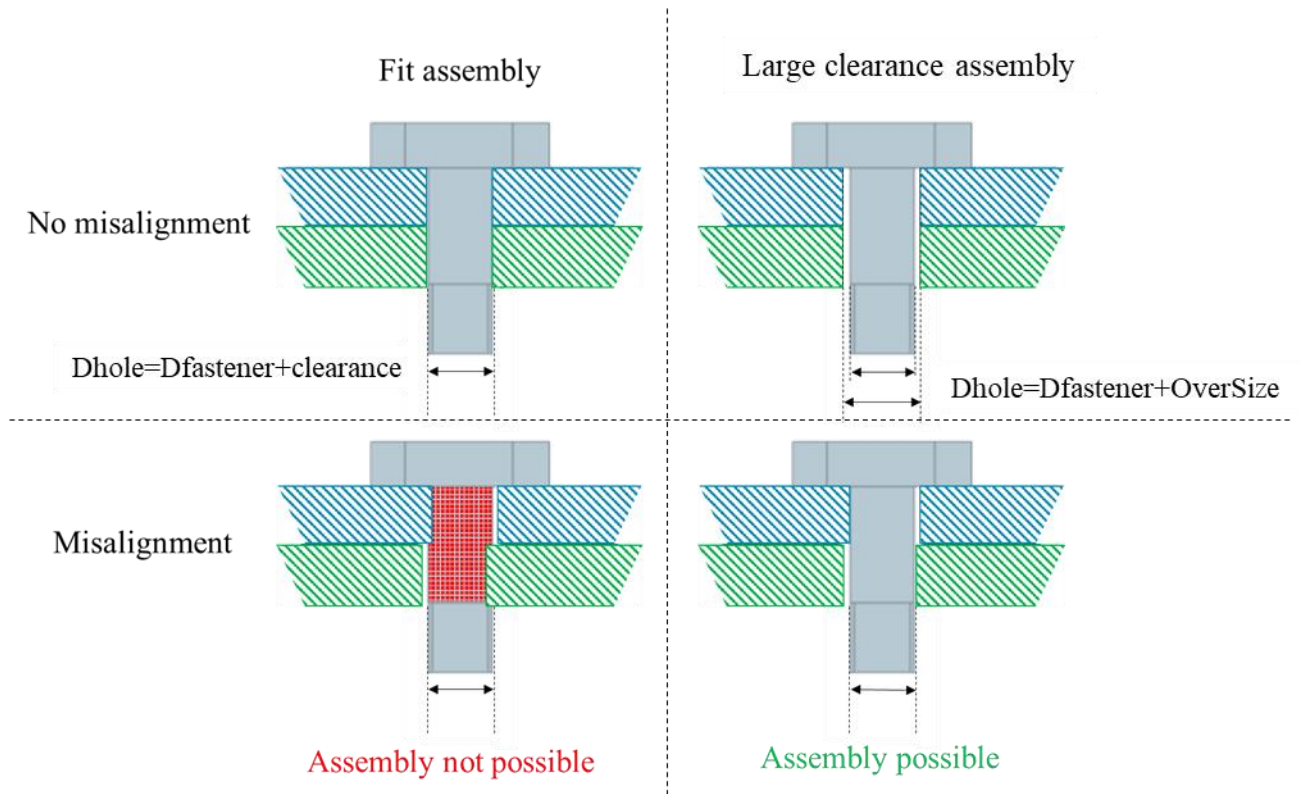
Figure 1 : Impact of Hole-to-Hole on bolt installation feasibility

D_{hole} and $D_{fastener}$ are respectively the diameter of the hole and the diameter of the fastener, while oversize (OS) stands for the augmented bolt-hole clearance linked to the H2H philosophy.

In this work Bloem studied the H2H assembly process under 3 axes: cost feasibility, technical feasibility and strength properties. Regarding cost analysis , he presents a cost calculation model to evaluate the potential gain brought by H2H trough recurring and non-recurring cost. Regarding technical feasibility, he shows a statistical tolerance model to determine hole positional and geometrical accuracy that can be then compared with expected accuracy from manufacturing. Finally regarding strength properties he gives the results from a physical test campaign investigating the effect of hole misalignment in riveted aluminum joints. His conclusions are the following, applying H2H assembly process with increased holes diameter leads to an increased static strength but a decreased fatigue life at lower load level. However very few details are given regarding tested misalignments value and global mechanical behavior.

Bolted joint behavior have been strongly investigated over the past decades to understand and determine the load distribution among different rows of fasteners and its effect on fatigue life. This last point is particularly critical regarding aircraft design as more than 60% of catastrophic accident in the civil aviation are linked to fatigue damage [5]. Such studies are both experimental and numerical [6-8]. Some similar investigations on bolt-hole clearance and error locations have been the topic of many publications, in particular in connection with composite laminates [9-15]. According to the latest publications, clearance and misalignments could potentially have a significant effect on the strength of composite bolted joints. To date however, very little quantified information has been published on the effect of hole misalignment on metallic bolted joint strength and fatigue life.

Furthermore, some structural parts, such as the pylon, are subjected to elevated temperatures. In such conditions, carbon fiber reinforced polymer (CFRP) or composites cannot be used because the heat has a harmful effect on their strength. In this case, metallic materials are needed, such as the titanium alloy Ti-6Al-4V, a material specifically developed for the aeronautic field, which has excellent mechanical properties and low volumetric mass density, and can be used over a wide range of temperatures [16].

Indeed industrial processes have a strong influence on the fatigue strength of bolted joint, as explained in the following publications [17-19]. Therefore they are widely use in the industry, however it would be wrong to assume that the benefits they bring is always compatible with H2H assembly philosophy. For example interference assembly is a joint configuration where $D_{fastener}$ is larger than D_{hole}. In such conditions the screw has to be inserted with force either by pulling or pushing it. The radial stresses thus installed in the joint strongly improved fatigue life. In H2H conditions the process rely on bolt hole oversizing thus making it not compatible. This paper addresses the issue of bolt-hole clearance and misalignment in bolted joints by means of an experimental study on Single-Lap Shear (SLS) specimens made of Ti-6Al-4V so

as to be representative of aeronautic junctions. The study presented here investigated the cross effect of various joint parameters: scale effect, specimen thickness and bolt preload. The analysis is focused on stress, strength and fatigue life of the tested joints.

2. Experimental methodology

2.1. Specimen details

For this experimental campaign, specimens representing SLS joints were tested. The reference geometry and hole numbering are shown in Figure 2. All specimen dimensions are linked to the nominal fastener diameter d, the value of which is 6.35 mm, unless stated otherwise for a specific testing case. The edge distance, e, the pitch distance p and the substrate length, L, were set to $2d$, $4d$ and $18d$, respectively. The width of the specimens depends on the loading case. In fatigue the objective is to assess the strength of the joint regarding net section failure. However, in static the studied failure phenomena are on the bolt bearing curve i.e. bolt shearing, plate bearing or bolt transition failure. Airbus test method suggest to set the width to $4d$ in fatigue, and $7d$ in static. A rapid comparison of resistant section can be done to verify this design. For net section the resistant section is $S_{NS}=t(W-d)$, with $t=d/2$ and $W=4d$ then the resistant section becomes $S_{NetSection}=3d^2/2$ which is inferior to the resistant section in shear for SLS joint with two bolts is $S_{Shear}=\pi d^2/2$,=. To insure bolt failure, the width must be increased from according 4d to 7d, which is consistent with comments from Dang Hoang [20]. Finally, the thickness, t, of both plates was linked to the test parameter t/d and will be discussed later.
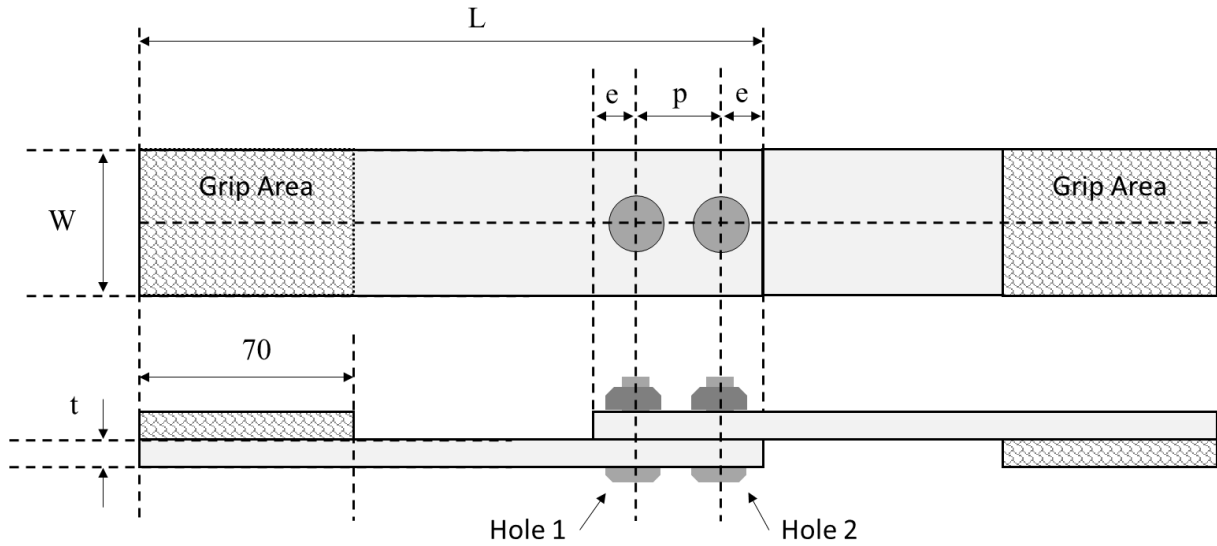
Figure 2 : Single lap specimen geometry with hole numbering.

This test campaign was intended to be representative of pylon structural assembly. The specimens were made of Titanium grade 5, Ti-6Al-4V Beta annealed, with the mechanical properties given in Table 1.

Property	Value
Young's Modulus (GPa)	114
Yield stress (MPa)	880
Tensile strength (MPa)	950
Poisson's ratio	0.34
Tensile nominal strain at failure (%)	15

Table 1 : Mechanical properties of Titanium Ti-6Al-4V

2.2.   *Fasteners used in the tests*

Two different fastener technologies were used in this study. Threaded fasteners are the most common fasteners in the aeronautic industry, so they were used here. However, the tightening process led to considerable uncertainty on the installed preload **[21]**. The preload corresponds to the clamping force applied to the plate by the bolt. It creates tension stress in the bolt and compression stress in the plates, and thus has an important impact on the pressure distribution at the joint interface, i.e. between the plates. This is why another fastener technology was also used: the swaged fastener. This type of fastener is installed by pulling on the stud end while a collar is mechanically deformed to create grooves resisting to tension. Such fasteners present

a smaller preload distribution than threaded fasteners, so the preload was better mastered in the tests involving this kind of fastener.

The threaded fasteners were composed of EN6115 Hi-lite screws, made of Ti-6Al-4V, and NSA5050 nuts, made of corrosion resistant steel (CRES). The swaged fasteners were composed of ABS0998 studs and ABS0999 collars, both made of titanium.

2.3.   Misalignment management

To investigate the impact of misalignments, several geometrical configurations were chosen. In this paper, the focus is on longitudinal misalignments, i.e. misalignments in the loading direction. Each misalignment configuration is identified by a capital letter and a number. The letter stands for the chosen geometrical misalignment configuration and the number stands for the hole diameter, OS. Each configuration can then be described by two parameters: the hole OS, which is the same for both the hole and the misalignment value. The misalignment value is a 2-uplet, one for each hole, defined in Figure 3 for one hole. It is noteworthy that, according to **Bloem [4]**, the value of hole misalignment must always be smaller than or equal to the hole diameter OS, otherwise fasteners cannot be installed. Figure 4 presents the different configurations tested and their identifications. Regarding manufacturing of the specimens, holes were drilled with NC machines in orbital drilling with an accuracy of ± 10 μm tolerance interval for their position and diameter values.
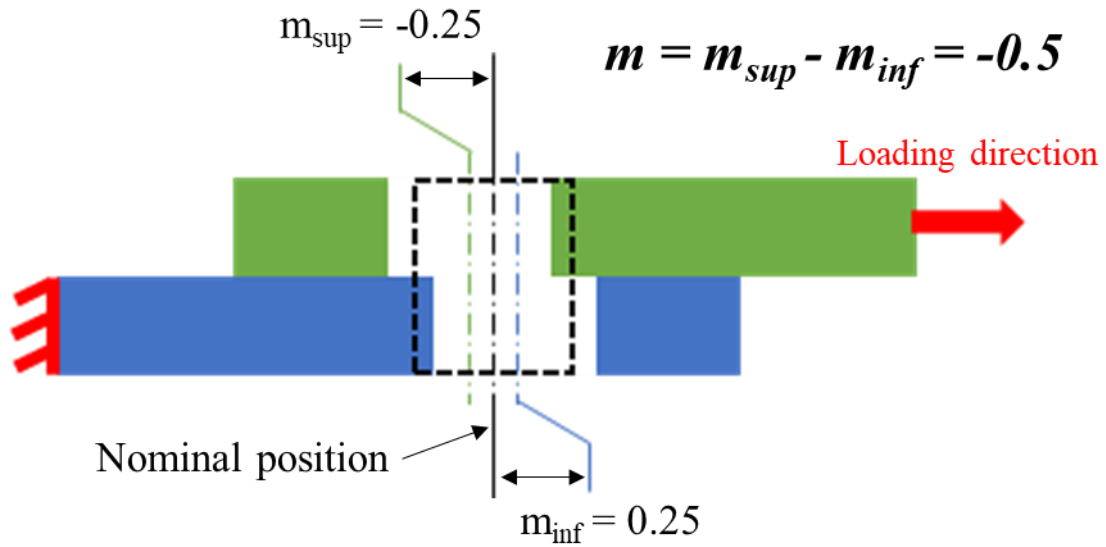
Figure 3 : Hole misalignment definition: m_{sup} represents the misalignment of the upper hole, m_{inf} represents the misalignment of the lower hole

2.1.4. Test parameters

The different misalignment configurations presented above were tested in different assembly conditions. The first parameter investigated was the fastener diameter, to observe potential scale effect. Two diameters were tested, d=6.35 mm and d=12.7 mm. It should be noted that specimen dimensions were larger in the case of larger bolts as the plate dimensions depended on the bolt diameter as described in section 2.1. However, misalignment values remained the same.
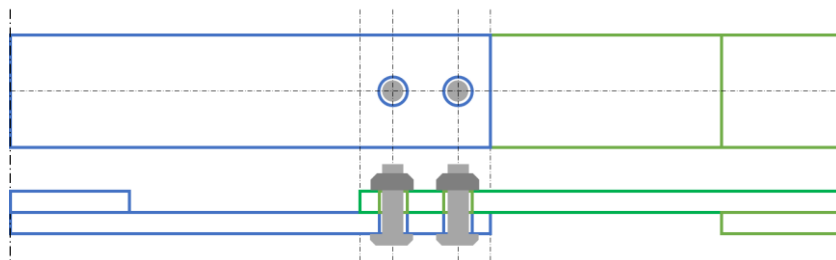
A0
$$OS_{A0}=0mm$$
$$m_{A0}=(0;0)mm$$
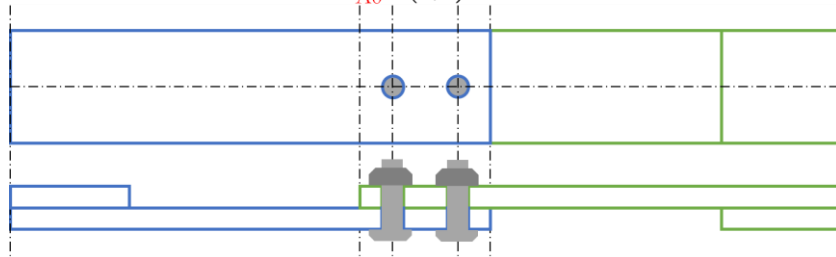
A5
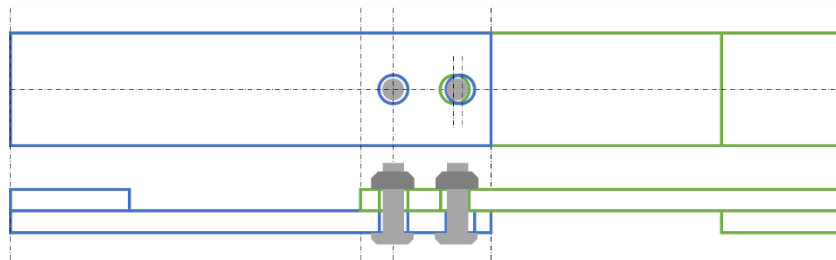$$OS_{A5}=0.5mm$$
$$m_{A5}=(0;0)mm$$

B5
$$OS_{B5}=0.5mm$$
$$m_{B5}=(0;-0.5)mm$$

C5
$$OS_{C5}=0.5mm$$
$$m_{C5}=(0;+0.5)mm$$
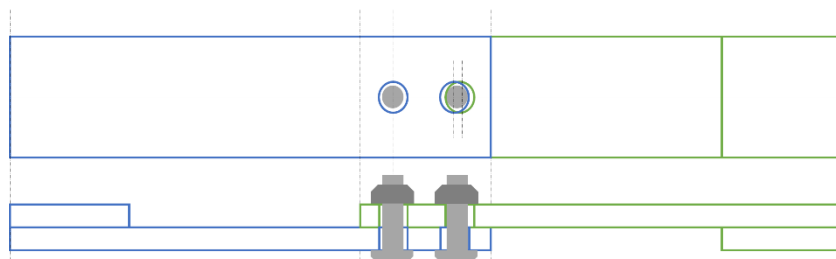
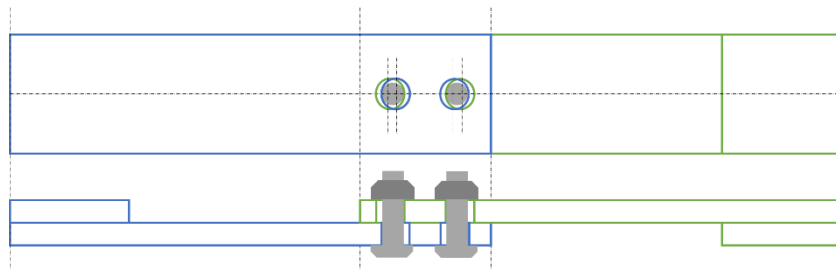**F5**
$$OS_{F5}=0.5mm$$
$$Ml_{F5}=(-0.5;+0.5)mm$$

Figure 4 : Hole misalignment configurations

The second test parameter investigated was the thickness of the plates. The ratio t/d is determinant regarding the static failure mode. So several t/d were evaluated to identify the effect of clearance and misalignments for different failure modes. The ratios tested were 0.25 and 0.5. Finally, the preload level was a parameter in this study. As explained above, both swaged and threaded fasteners were used in the tests presented. While swaged fasteners have a unique and repeatable preload when they are installed, threaded fasteners can be tightened at different torque levels, thus leading to different load levels. In this paper, the preload level P is defined as the ratio of the clamping load ($F_{clamping}$) induced by tightening, to the ultimate tensile strength (UTS) of the fastener:

$$P(\%) = \frac{F_{Clamping}}{UTS} \times 100$$

Equation 1 : Preload formula

This formula is proposed in this paper as a simplification of the clamping force. Thus, no particular measurement device were used to monitor the installed bolt load. Furthermore, due to several phenomenon during torque tightening, such as variation of friction coefficient and different deformation of the nut, the targeted clamping load is difficult to achieve in industrial context, as illustrated in Figure 5. Instead a range of clamping force is given defined as a percentage of the Ultimate Tensile Strength of the fastener, usually centered around 50%.

For a swaged fastener, the preload is induced by the deformation of the collar and its level is generally set at around 65% of the fastener's ultimate tensile strength. For threaded fasteners, torque tension tests are performed to evaluate the torque needed to reach 25%, 50% and 75% of the fastener's ultimate tensile strength. In lab conditions the clamping load discrepancy is reduced in comparison to manufacturing. However there were no study of uncertainty in the allied load in this study.
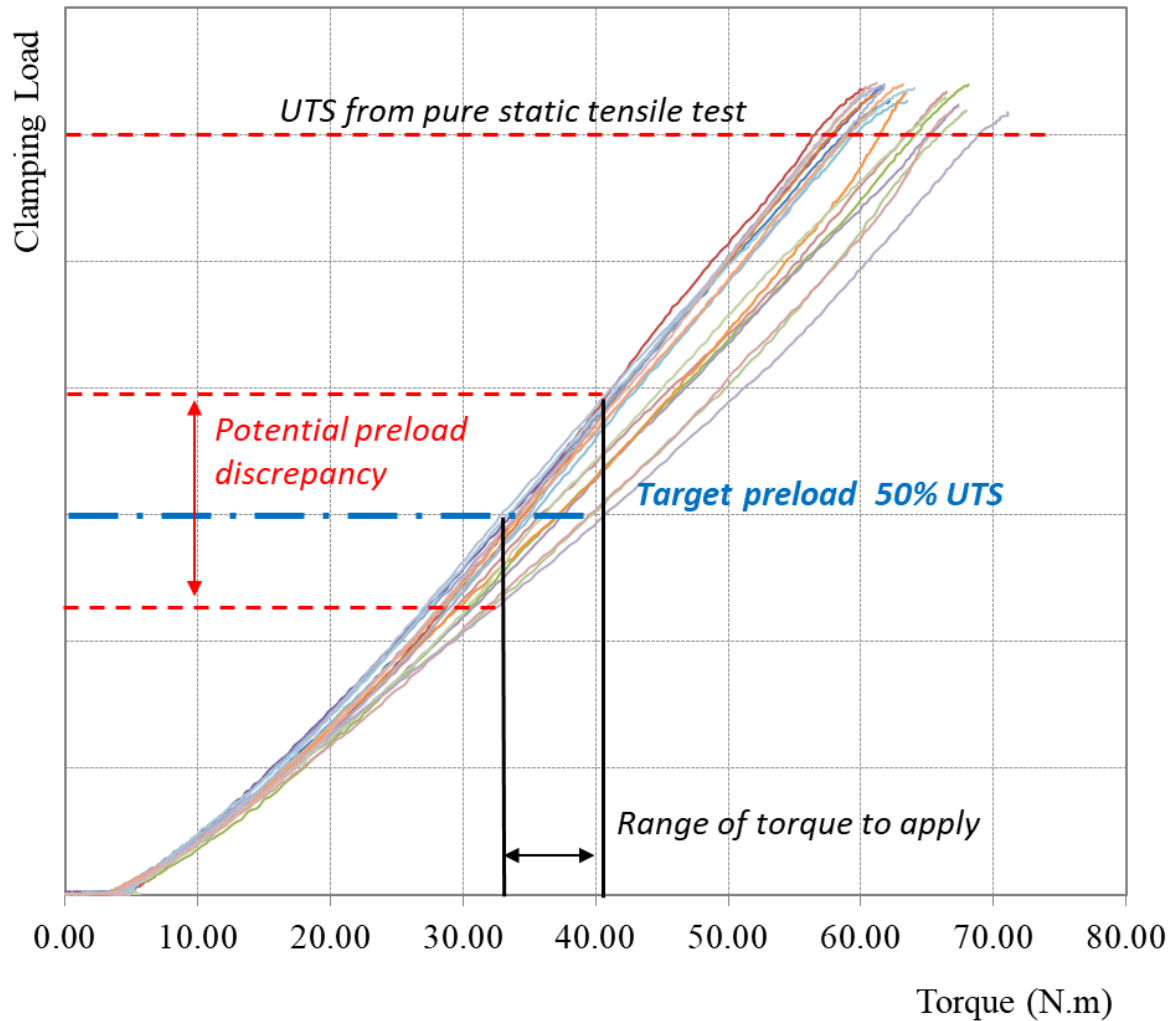
Figure 5 : Preload variation during torque tightening of a threaded system

During the fastening process of the specimen, the position of both plates and bolts was essential for this particular test campaign as positions were referred to test parameters. To achieve good accuracy, specific centric pins were designed and machined to ensure the best possible relative positioning of plates.

The centring pins were inserted into the plate holes with a clearance of less than 10 µm. Then, a clamping tool was used to lock the plates in the right position. Finally, the bolts were installed once the centring pins had been removed.

Table 2 presents the test matrix of this study. **Table 3** compares the different tests and notes the associated effect studied through this comparison.

TEST	t/d	d (mm)	Fastener type	P (%)	Misalignment Configurations	Static	Fatigue
1 (Baseline)	0.5	6.35	Swaged	50%	*A0, A5, B5, C5, F5*	yes	yes
2	1	12.7	Swaged	50%	*A0, A5, B5, F5*	yes	no
3	0.5	6.35	Threaded	25%	*A0, A5, B5, F5*	yes	yes
4	0.5	6.35	Threaded	75%	*A5, F5*	yes	yes
5	0.5	6.35	Threaded	50%	*A5, F5*	yes	yes
6	0.25	6.35	Swaged	50%	*A0, A5, F5*	yes	no

Table 2 : Test matrix

Cases Compared	Effect studied
1 vs. 2	Bolt diameter
1vs. 6	Thickness of plates
3 vs. 4 vs. 5	Bolt preload

Table 3 : Tests compared and the effect studied

2.2. *Test method*

2.2.1. *Static testing procedure*

Static tests were carried out on a hydraulic test machine with capacities from 0 to 250 kN. A displacement was imposed with a test speed of 0.5 mm/min until the specimen failed. The reaction load from the test machine and the displacement of the hydraulic actuator were measured and recorded during the loading phase to provide load vs. displacement curves. Repeatability was assessed using three specimens per test case.

2.2.2. *Fatigue test procedure*

Fatigue tests consisted of the application of a sinusoidal monotonic load, with a ratio $R = \sigma_{min} / \sigma_{max} = 0.1$. The frequency was set to 10 Hz and the tests were carried out at ambient temperature on hydraulic machines (capacity: ±100 kN to ±250 kN), as shown on Figure 6. The value of the external force was chosen so as to characterize the fatigue strength of the joint in the fatigue life range of 10^4 to 2.10^6 cycles. Static tests conducted previously helped to determine the values of the initial external load to be applied in fatigue tests. Finally, fatigue tests were performed according to standard NASM1312-11.

The physical test campaign as described in this paper has a large number of parameters to evaluate, and using more test coupons would have strongly increased the cost of this campaign. There are two approaches to handle the effect of scatter in fatigue results. The first option is to test several coupons at the same load for 3 different load level. The second option, chosen in Airbus test method, is to test 1 coupon for each different load level with a minimum of 8 coupons test, at least one of those shall not reach failure under 2.10^6 cycles. The scatter of results is then distributed at each load level thanks to the interpolation of the S-N curves as shown in the work from **Ramière et al.** [22].

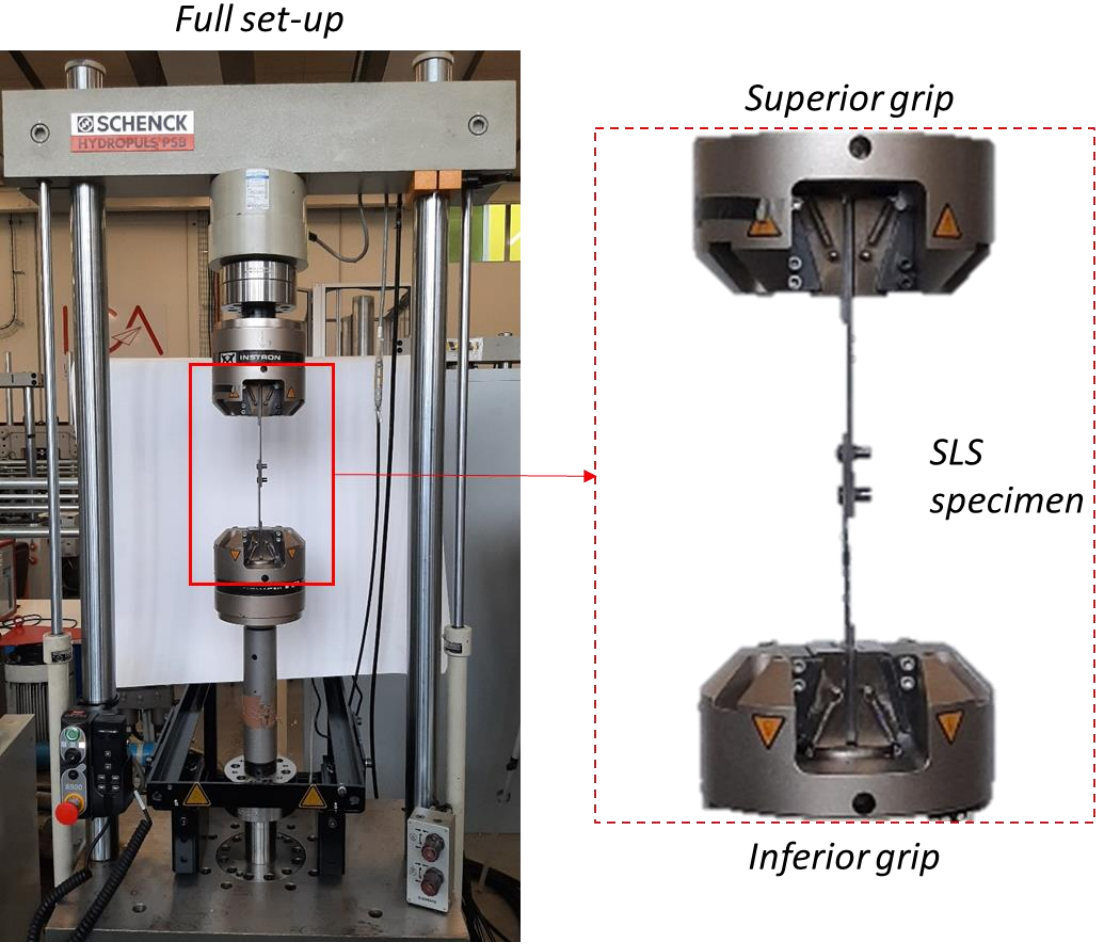The results observed were S-N curves (maximal stress (MPa) vs. fatigue life (cycles)), also known as Wohler curves.

Figure 6 : fatigue test set-up

3. Experimental test results for baseline assembly conditions

3.1.   Static test results

3.1.1. Load vs. Displacement curves

The load is shown as a function of the applied displacements in Figures 7 to 11 for each of the 5 test configurations. For configurations with OS or misalignment, the reference curve (A0) is also represented (solid red line) to make differences easier to observe. The loads reported on all the curves are normalized with respect to the maximal force recorded for the case A0. For greater clarity, the figures show the most representative specimen for each case. However, the maximal strength of each specimen is summarized in Table 4 and those results show excellent repeatability.

Guillot [23-24] proposed a synthesis describing the different phases of behaviour for a bolted joint under quasi static loading. His description concerns bolted joints with low clearance and low tightening level. He describes the loading behaviour of those specimens with three stages: first a stage of friction, then a stage of elastic deformation and, finally, the stage of plastic deformation leading to failure.

In stage one, the load has to overcome the friction due to the bolt tightening. At this point, there is no contact between the plates and the bolt shank. All load vs. displacement configurations are gathered together in Figure 12, where it can be observed that the friction zone is similar for all misalignment configurations. Then the titanium plates slide on one another until contact is made between the hole of at least one of the plates and its bolt shank. For the configurations *A5* and *B5*, it can be observed that sliding begins and ends at similar displacement values from 0.2 to 0.8 mm. However, there is no visible sliding for the configurations *A0*, *C5* and *F5*. For *A0*, the 30 μm clearance is too small for sliding to be observed. For *C5* and *F5*, the misalignment of hole 2 induces direct contact of the fastener such that no sliding of the plates is possible.

Despite the lack of visible sliding, the change of slope in the load displacement curves indicates the transition from the friction zone to the elastic deformation zone.

This following zone is a quasi-linear elastic deformation zone. The global stiffness of the assembly results in the slope of this elastic zone. It can be observed that the slopes are very similar for configurations *A0* and *A5*: respectively 0.62 and 0.59 mm^{-1}, while the slope is lower for the other misalignment configurations (around 0.4 mm^{-1}). In a similar way, this zone reaches a higher load level for configurations *A0* and *A5* (around 0.68) than for misaligned configurations (around 0.45).

The final zone is a non-linear plastic deformation zone. Once again, quasi-parallel behaviour can be observed between configurations *A0* and *A5* on Figure 8, whereas an uncommon phenomenon can be observed on Figure 9 and Figure 10**:** on the configuration *B5* and *C5,* a particular point, named shifting point on the figures, can be identified, where the slope of the curve which was previously decreasing, starts to increase again. This behaviour is visible on those two configurations only, and it can also be noted that it occurs at a similar load level of 0.55. The end of this final phase is the failure of the specimens.
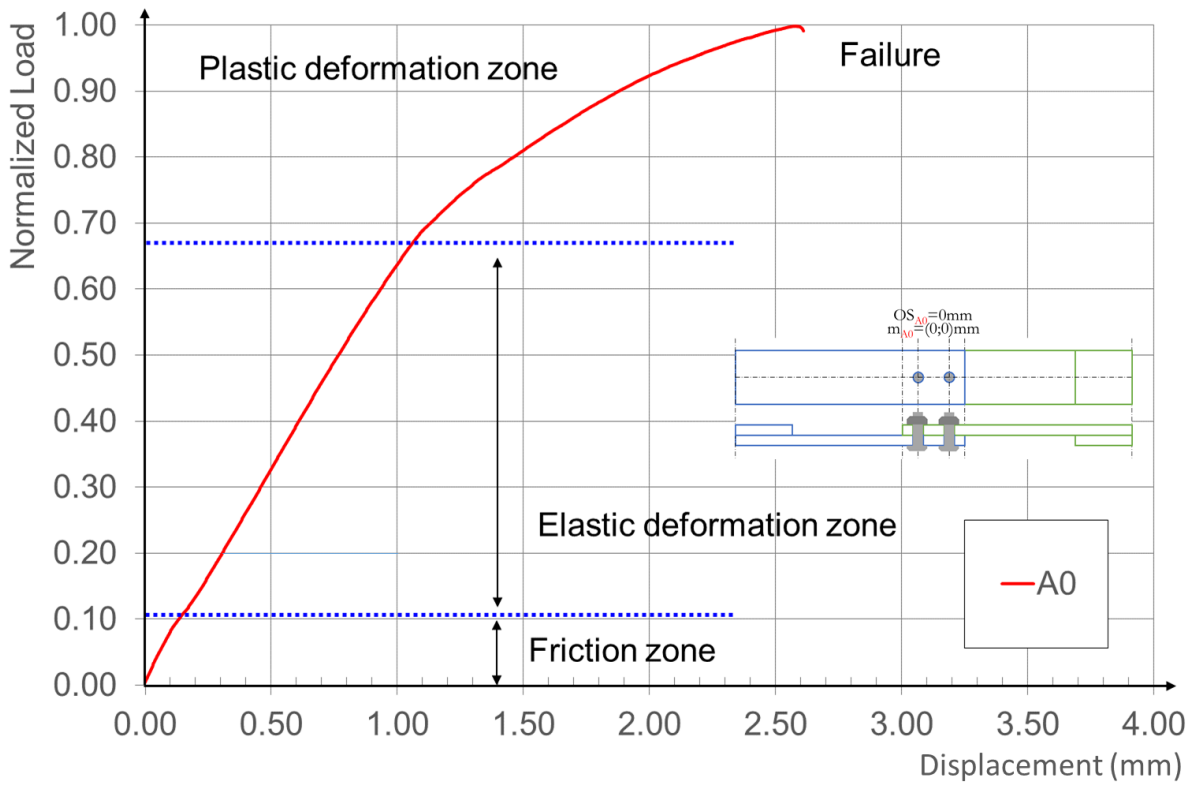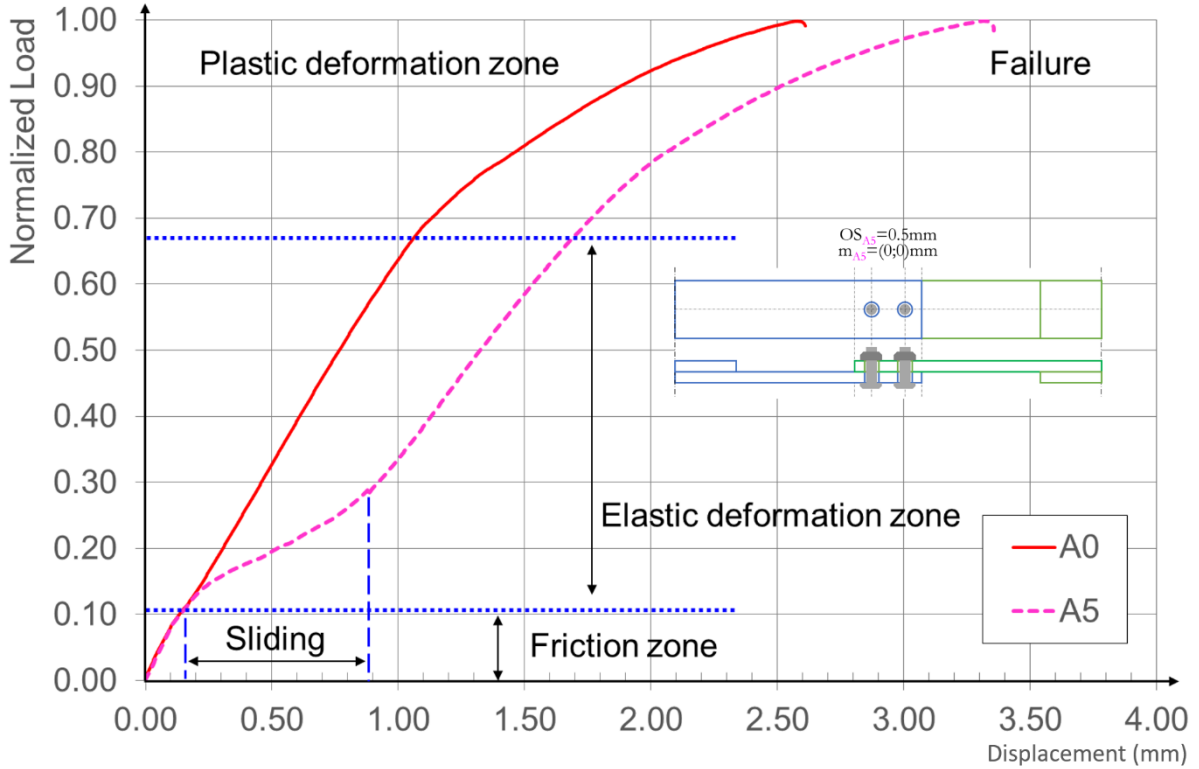
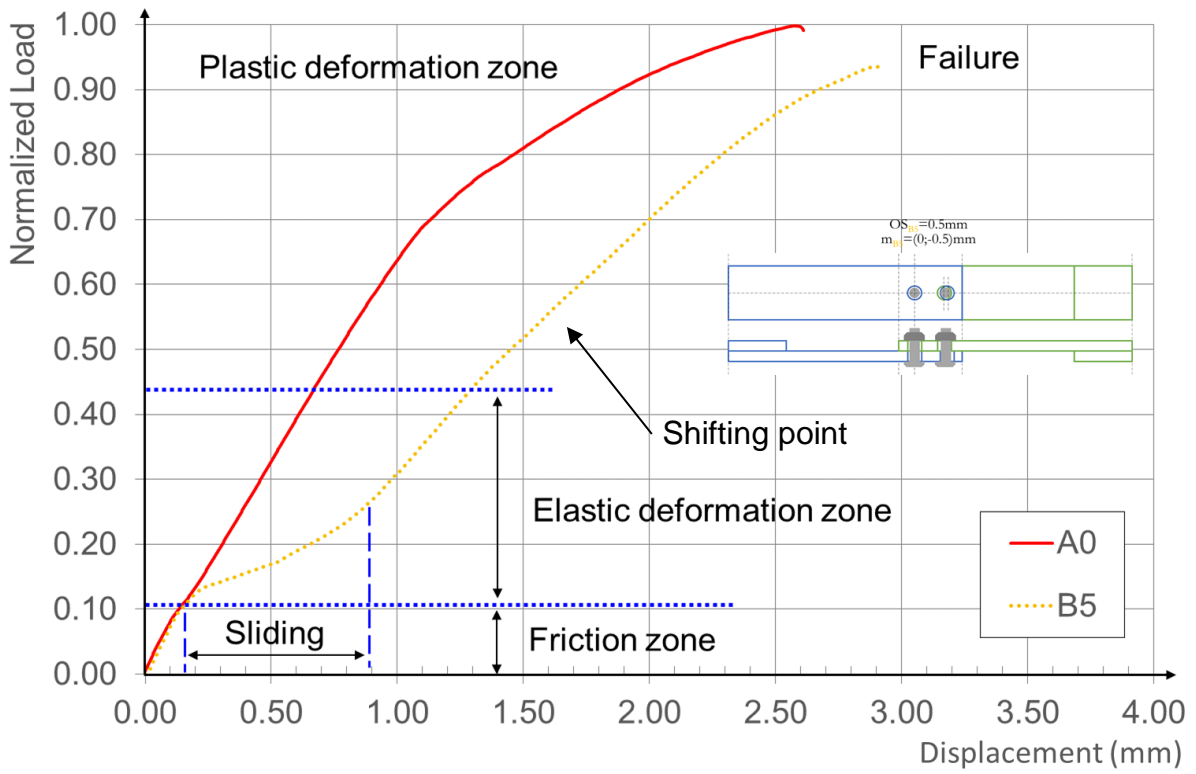**Figure 7 : Load vs. Displacement A0**

Figure 8 : Load vs. Displacement A5
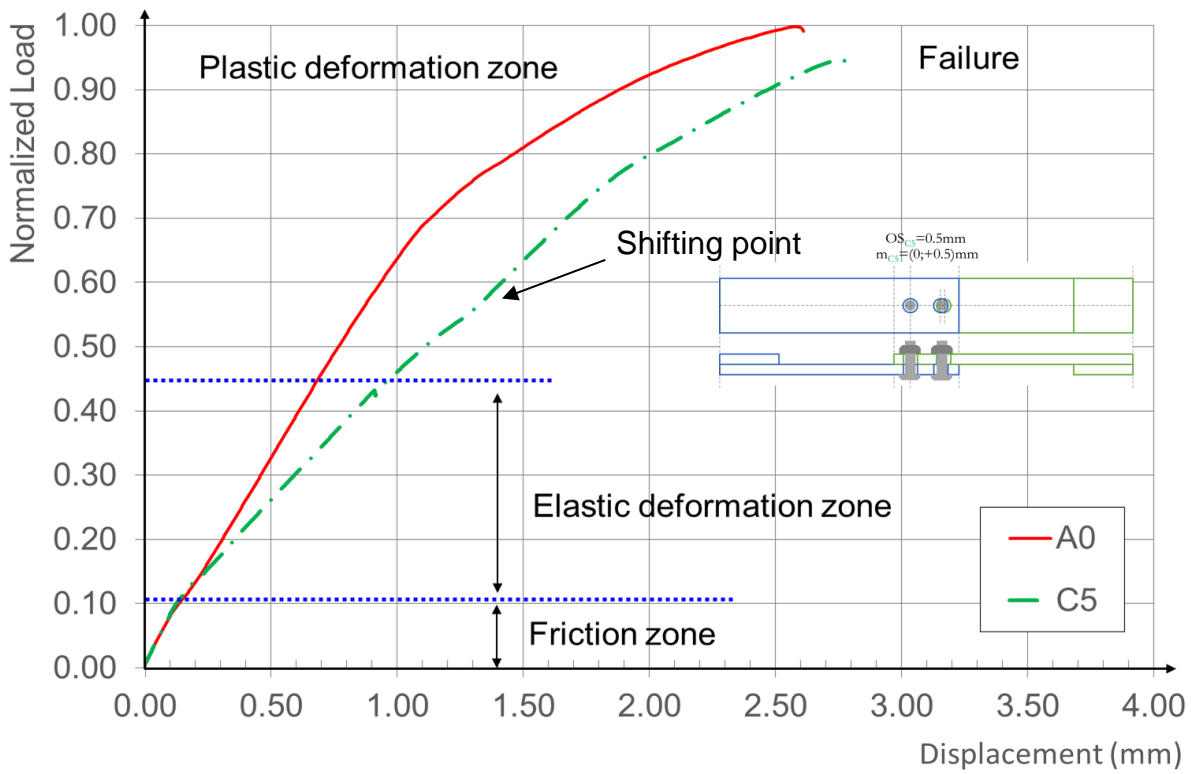
Figure 9 : Load vs. Displacement B5

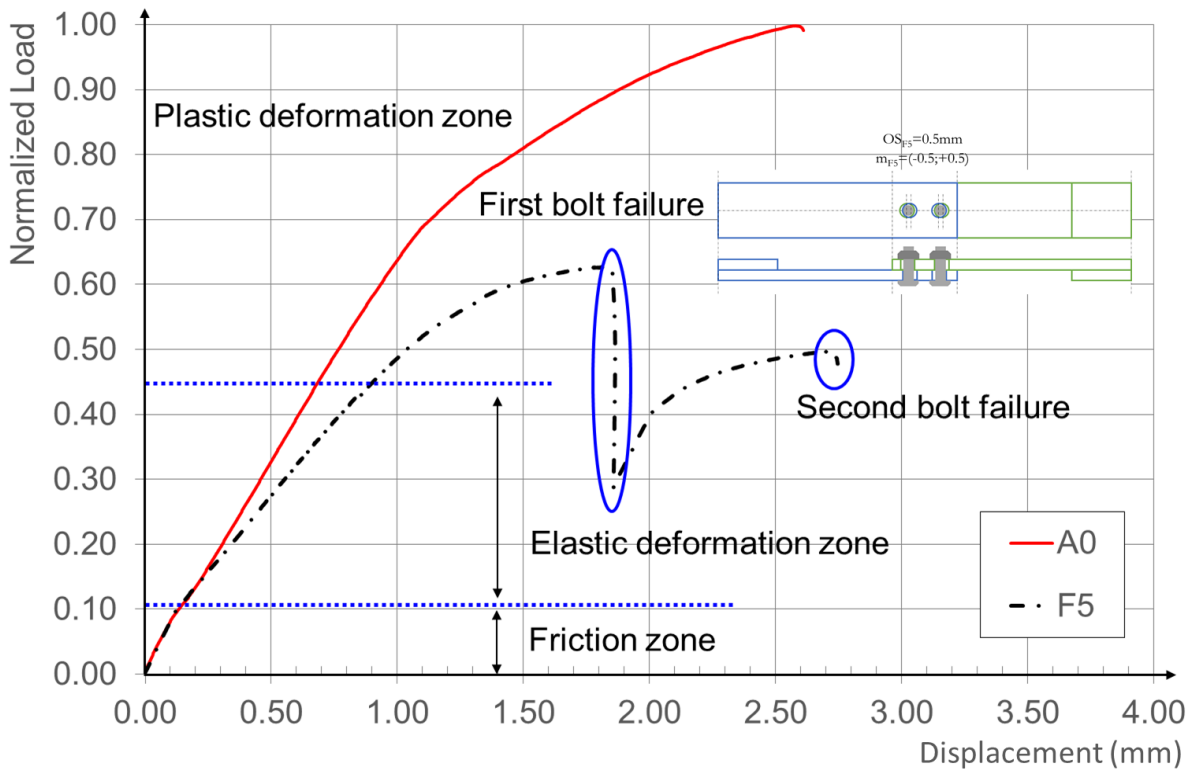**Figure 10 : Load vs. Displacement C5**
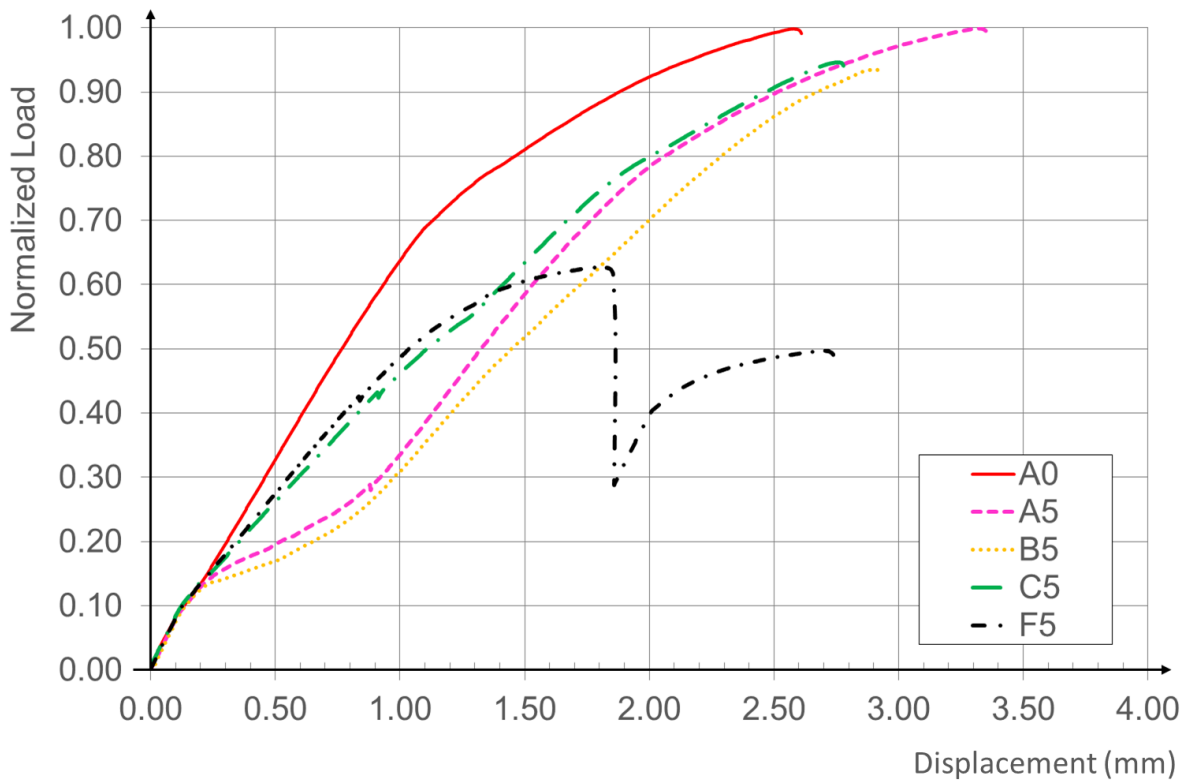
Figure 11 : Load vs. Displacement F5

Figure 12 : Load vs. Displacement Baseline test

3.1.2. Static Failure mode and level

The failure mode for the baseline test was bolt shank shearing; the remaining states of both bolts after failure are shown in Figure 13. The shearing plane is perpendicular to the bolt axis and corresponds to the interface plane between the two plates of the assembly. It can be seen that failure of bolts is simultaneous for every misalignment configuration except for *F5*. In this particular configuration, it was observed in real-time that the fastener in the 2nd hole was violently ejected after its failure and, at the same time, a large decrease occurred in the load (-0.34). However, the load increased again, since the remaining bolt did not fail.

The maximum strength of each specimen and a comparison with reference A0 are summarized in **Table 4**. By comparing the configurations *A0* and *A5* it can be concluded that the clearance has no impact on the static strength of the assembly. However, a decrease of the maximal load before failure is observed on the configurations *B5*, *C5* and *F5*. For the configurations *B5* and *C5*, the maximum load transmitted is observed immediately before simultaneous shearing of bolts and, in both cases, it reaches 0.94 of the normalized load. A much stronger decrease is observed for the configuration F5, where the maximal load occurs immediately before the failure of the first bolt (hole 2) and reaches 0.63 of the normalized load.
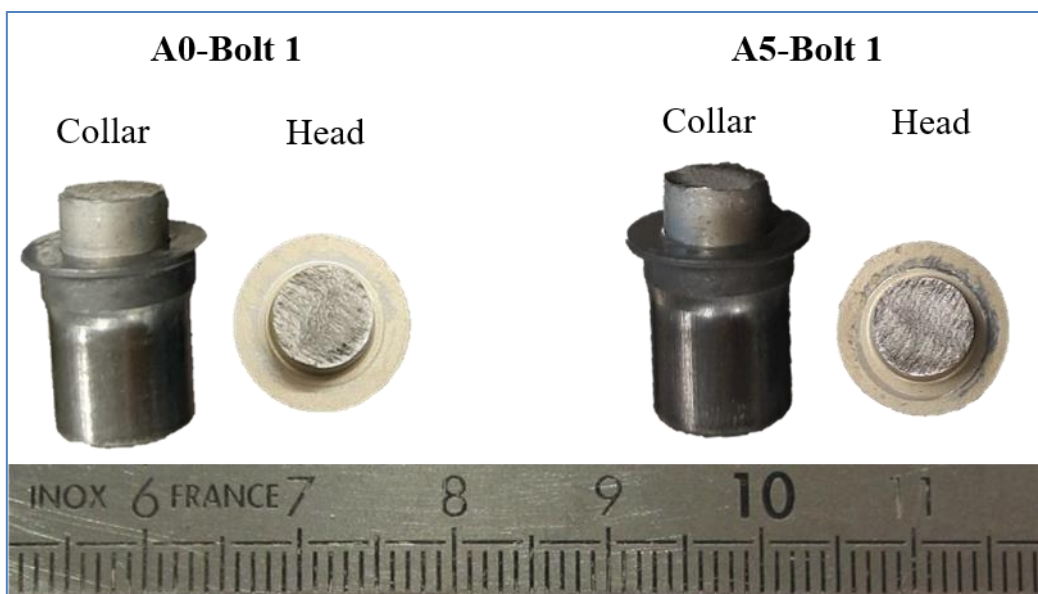

Figure 13 : Bolt shear failure surface Bolt 1 from configuration A0 and A5

Configuration	A0	A5	B5	C5	F5
Max Strength Specimen 1	0.99	1.00	0.93	0.93	0.63
Max Strength Specimen 2	1.00	1.00	0.94	0.93	0.63
Max Strength Specimen 3	1.00	0.99	0.94	0.95	0.64
Max Strength Mean	1.00	1.00	0.94	0.94	0.63
Variation (%)	-	0.00%	-5.69%	-6.02%	-36.4%

Table 4 : Baseline tests maximal static strength and comparison against A0

3.2. Fatigue test results

3.2.1. S-N curves and Key Fatigue Indicator

The results of the baseline assembly fatigue tests are shown in Figure 14. The different points represent the raw data from the tests while the curves result from interpolation under the assumption of a power law. The reference curve *A0* (solid red) globally presents the longest fatigue life. A decrease in fatigue life can be observed on the clearance and misaligned configurations. The main result observed is the Key Fatigue Indicator (KFI). This corresponds to the maximal normal stress from the interpolated curve at 10^5 cycles. This indicator is normalized so that the KFI on the configuration *A0* is 1. The KFI for each configuration tested and its comparison against the configuration *A0* are presented in **Table 5**. It can be seen that configurations with marked sliding behavior (*A5*, *B5*) show a lower decrease of KFI, of around 6-7%, than configurations with low sliding behavior (*C5*, *F5*), around 12-13%.

Indeed, a correct evaluation of the fatigue behaviour cannot be assessed by focussing to the KFI only. This is why the full Wohler curves are presented. However, in this study each configuration's curve appears to have similar slope. So it is acceptable to only discuss the results at the KFI level.

Configuration	A0	A5	B5	C5	F5
KFI (10^5 cycles)	1.00	0.94	0.93	0.88	0.87
Variation (%)	-	-5.69%	-6.69%	-11.7%	-12.7%

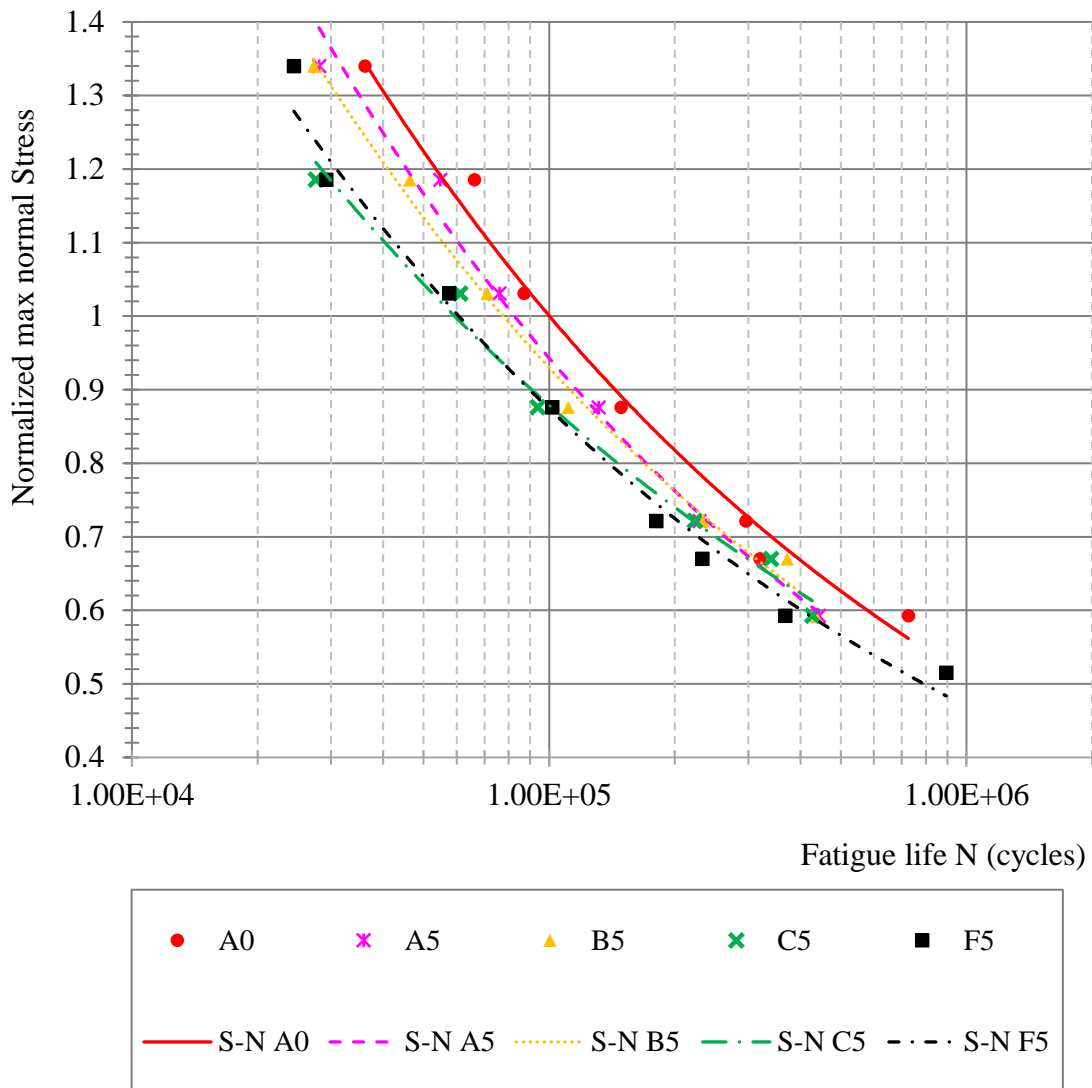**Table 5 : KFI for baseline tests and comparison against A0**

Figure 14 : Fatigue results test 1

3.2.2. Fatigue failure mode and location

For this test campaign, the specimens were designed so that the failure in fatigue occurred within the plates. An analysis of the failure profile helped to understand where the fatigue failure started. Usually, for low levels of preload, the failure occurred in the net section of the specimen. Benhaddou et al.**[21]** have also shown that higher levels of preload shift the initiation point slightly outside the bolt hole. The most representative failure location for each configuration, i.e. the failure occurring for a majority of coupons, are shown in Figure 16. For the configurations A0 and A5 the failure is shifted from the hole and lies on the collar side, this

is consistent with the observations from Benhaddou et al.**[21]**, and it is due to strong compressive stress in the joint due to the bolt preload, it can be observed that this failure presents the longest life strength. For the configuration B5 the failure is on the head side of the bolts and begins outside the bolt hole, this change of side is mainly due to hole misalignment as it affects the stress concentration and generate more damage in this area of the joint. For the configurations C5 and F5, the failure starts on the collar side of the bolts but the fastener shank is visible. The difference of failure location may be explained by once again by the holes misalignment.

The failure analysis of the microstructures bring generally a lot of information such as the origin point of the failure and the number of fatigue cycles for the propagation up to final static failure. However, in this case as the material is Titanium Ti-6Al-4V Beta annealed, the microstructures is made of rather large grain making the failure profiles hard to analyze and the counting of stries impossible, as shown on Figure 15.
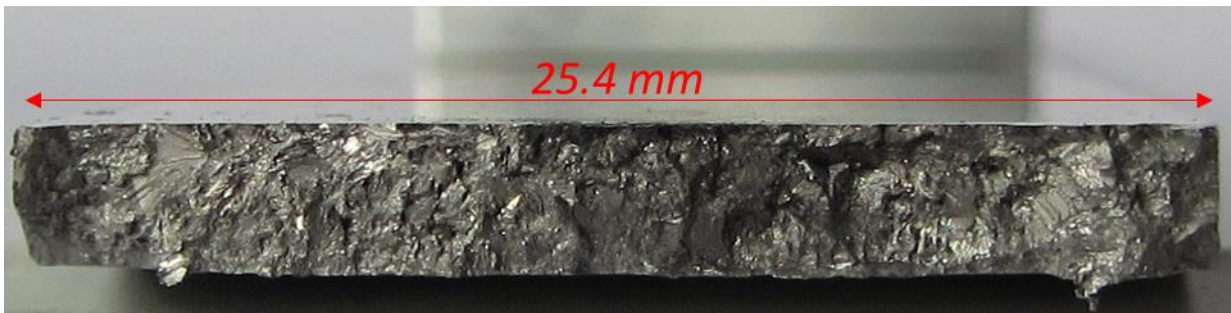

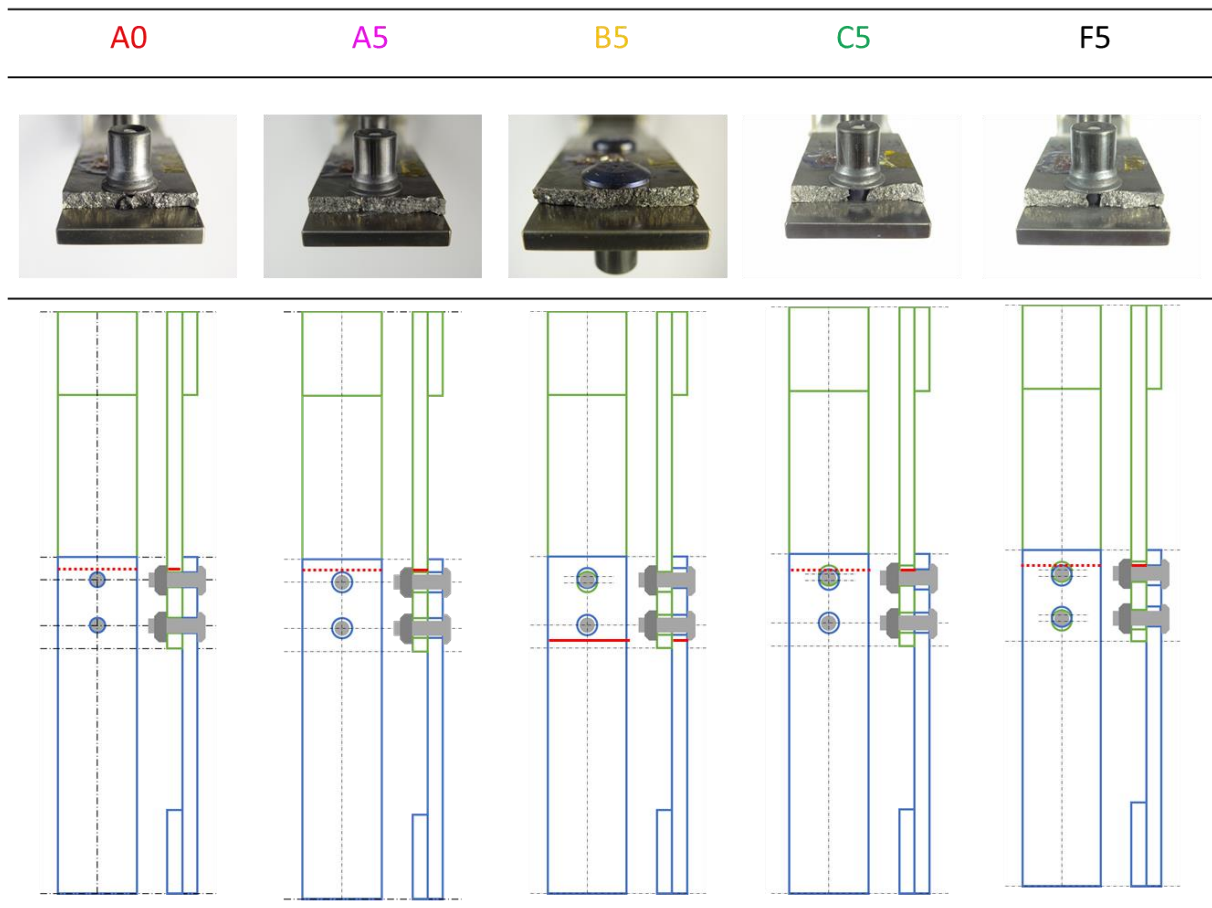**Figure 15 : failure surface A0 specimen 1 (green plate)**

Figure 16 : Representative fatigue failure location

3.3 Conclusions on baseline assembly tests

Regarding the static behavior and strength, the bolt hole clearance (*A5*) creates a sliding phase between the friction and bearing phases. However, it impacts neither the stiffness of the joint nor its strength. The misalignments of bolt holes can also create this sliding phase (*B5*) but do not necessarily do so (*C5* and *F5*). However, the stiffness of the joint is strongly decreased in the bearing phase and, finally, the maximal strength of the joint is also impacted. It can be observed that, when the misalignments occur on only one of two bolt holes (*B5*, *C5*), the decrease in strength is less severe than when there are opposite misalignments on both holes (*F5*). The displacement needed for contact of both fasteners is indeed shorter for configurations *B5* and *C5* than for *F5*.

Regarding fatigue life, bolt hole clearance has a low impact – around a 6% decrease compared with the reference joint. It can be observed that this geometric configuration promotes initiation of the failure in the plate on the collar side. The misalignments have different impacts depending on the position of the first bolt in contact. For the configuration *B5*, contact occurs first in hole 1, in contrast to what happens in configurations *C5* and *F5*. The misalignments also decrease the fatigue life of bolted joints and, once again, the strongest misalignments tested in the configuration *F5* show the worst KFI, with a decrease of 13%.

4. Comparative analysis with different joint parameters

The second part of this experimental study aimed to identify the impact of different assembly parameters in presence of clearance and misalignments.

4.1. Effect of bolt diameter

The effect of bolt diameter is considered in this section by comparing test case 1(baseline) with test case 2. In the first test case, the fasteners had a diameter of 6.35mm while, in the second, their diameter was 12.7mm.

The load displacement curves recorded during static loading tests until failure, for configurations *A0*, *A5*, *B5* and *F5*, are shown in Figure 17. The load needed to reach failure is much higher in specimens with larger bolt diameters. However, the normalized value remains as provided by the baseline test, so the load level can still be compared.

The friction zone is similar for the different configurations tested for both bolt diameter cases. Then, the sliding phase occurs on configurations *A5* and *B5* while a slope change can be seen for the configurations *A0* and *F5*. Next, the elastic deformation zone can be observed. As for test case 1, the elastic phase reaches a higher load level for configurations without misalignments, *A0* and *A5*. Then the plastic deformations start, characterized by a strong displacement with slow load evolution. This phase ends with the failure of the specimen.

For the configurations with misalignments, *B5* and *F5*, the plastic deformation zone starts earlier. As for smaller bolts (case 1), the configuration *B5* has a shifting point in its loading behavior. However, configuration F5 now presents a shifting point, which was not present in tests with smaller bolts.

Regarding the failure of the specimens, the mode occurring here is bolt shearing, which is similar to the case with smaller bolts. Final failure occurs simultaneously on both bolts of the specimens for all H2H configurations, except for the strongly misaligned configuration *F5*. Table 6 shows the maximal load reached before failure and the variation against the configurations without defect, *A0*. The configurations with clearance (*A5*), reach the same value as A0 whereas misaligned configurations reach a lower level. However, the variation compared to A0 is lower than in the case of smaller bolts: for configuration *F5,* there is a link between the new behavior during loading and the final load reached before failure.

The conclusions that can be drawn from this test case are the following:

- The scale effect has no impact on the behavior of assemblies with clearance or low misalignment values.

- When the misalignment value is large, increasing the bolt diameter helps to decrease the loss of strength induced by misalignments

Configuration	A0	A5	B5	F5
Max Normalized Load before failure	4.22	4.20	4.12	3.41
Variation (%) against A0	-	-0.47%	-2.37%	-19.2%

Table 6 : Maximal static strength in baseline tests and comparison against A0
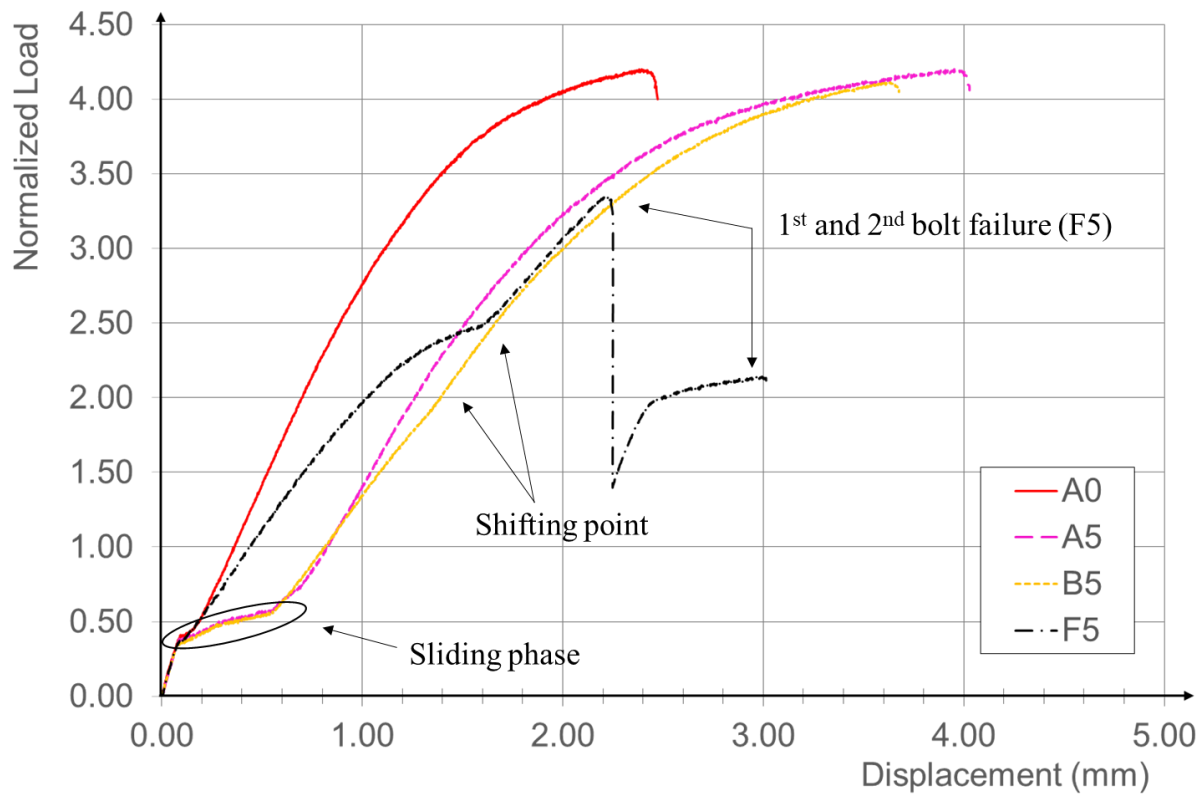
Figure 17 : Load vs. Displacement with 12.7 mm diameter bolts

4.2   Effect of substrate thickness

The effect of subtract thickness is considered in this section by comparing test case 1 (baseline) with test case 3. In the first test case, the thickness of each plate was 3.175 mm, while in the third, the plate thickness was 1.58 mm.

The thickness of the plates is a design parameter that is really important regarding not only the mass but also the structural strength. The ratio t/d is directly linked to the failure mode of a bolted assembly. Depending on this parameter different design calculation must be performed **[24;26]**. During the first phase of the test campaign the thickness ratio studied was 0.5 and its corresponding failure mode was bolt shearing. To evaluate the impact of a different failure mode, the thickness ratio was decreased to 0.25. The observed failure mode for this thickness ratio was plate shearing as shown in Figure 18. The post mortem observation of specimens did not show any deformation on the fastener. However, large bearing deformations could be seen, leading to final failure in shear-out. Large out-of-plane displacements were observed along with

26

a rotation of the fasteners around the transverse axes. This rotation is referred to as tilting of the bolts in the descriptions below.

The load vs. displacement curves recorded during the static loading tests of the different configurations are shown in Figure 19. The normalized value remains the same as in Figures 6 to 10. Regarding the reference curve (*A0*: red), it can be observed that the loading phases are similar to those of the baseline test. However, the failure occurs at a higher displacement value and the ultimate load is lower (0.86) as the large deformation in the plate appeared during the plastic zone deformations.

Configuration *A5*, representative for clearance, presents expected slipping behavior. Its strength is 0.8, slightly lower than that of configurations *A0*. It can be observed that the bolts rotations is greater in this configuration than in the configuration *A0*. These observations tend to explain the loss of strength as the plate was more stressed in out-of-plane shear as well as in bearing.

Both configurations *B5* and *F5* present a strength of 0.8, similarly to *A5*. The strong deformation in the plates allows the load to be redistributed among the two fasteners despite misalignments. So the loss of static strength is less severe in this failure mode for configurations *F5*.

The conclusions that can be drawn from this test case are the following:

- A thickness ratio t/Ø lower than or equal to 0.25 leads to strong bearing deformation that finally results in shear-out failure in the assembled coupons.

- Bolt hole clearance allows bolt rotation, inducing out of plane stresses. Small plate thicknesses are more sensitive to out-of-plane deformation reducing the strength of the joints.

- Strong misalignments have little impact on joint strength when the failure mode is plate bearing rather than bolt shearing.

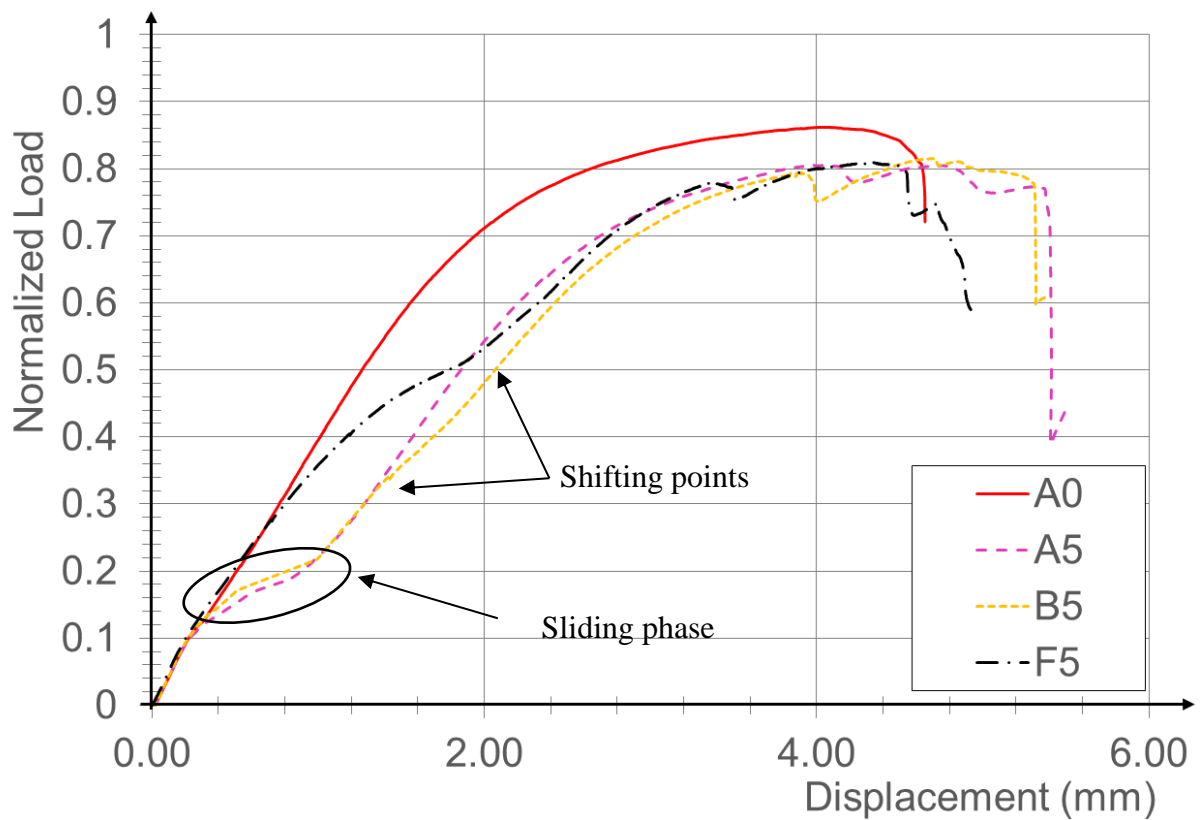**Figure 18 : Representative failure of a specimen with small thickness**

Figure 19 : Load vs. displacement of a specimen with small thickness

4.3. Effect of bolt preload

4.3.1. Impact of bolt preload on static behavior and strength

The static load vs. displacement curves for similar titanium bolted assemblies at different bolt preload levels are shown in Figure 20. The configuration *A0* was tested at two preload levels, 25% and 50% of the UTS of the bolt. The test results (Figure 20, a) show no impact of preload level on either the behavior or the maximal load before failure for this reference configuration. For configuration *F5*, the joint strength remains similar at different bolt preload levels. Finally, for configuration *A5*, the bolt preload does not have any effect on the maximal load before failure. However, it seems to strongly impact the behavior of the configuration, specifically in the sliding area. At a low preload level, the sliding occurs at a constant loading value (0.08). For a medium preload level, sliding starts at the same level but the load increases during this phase. For a high preload level, sliding starts at a higher loading level (0.16), and presents the same behavior as for the medium preload level: the two curves are the same. As a result, bolt bearing initiates at different load and displacement levels. However, it impacts neither the plastic deformation zone, nor the final failure.

The observed results in this study are different from the ones presented by **Rodrigues et al. [27].** In the work from Rodrigues the slipping behavior is slightly different as it occurs on two noticeable loading level. Never such a behaviour was observed during the presented physical campaign. Indeed, the numerical analysis from Rodrigues was made on Double-lap-shear specimen, during the first slipping phase only the middle plate moves so the global load is only submitted to the friction at the plate interfaces, then both the bolt and the middle plate are moving so the friction load is the addition of the friction at plate interfaces and under the head ant the nut of the bolt, see Figure 21. For a single-lap-shear specimen such a decomposition could also exist but in this case the friction load of the two phases are very similar. This might explained why the two phase behaviour was not observed in the presented tests. Furthermore

the secondary bending may influence the slipping phase and generate the observed increase of friction load during the slipping as observed.
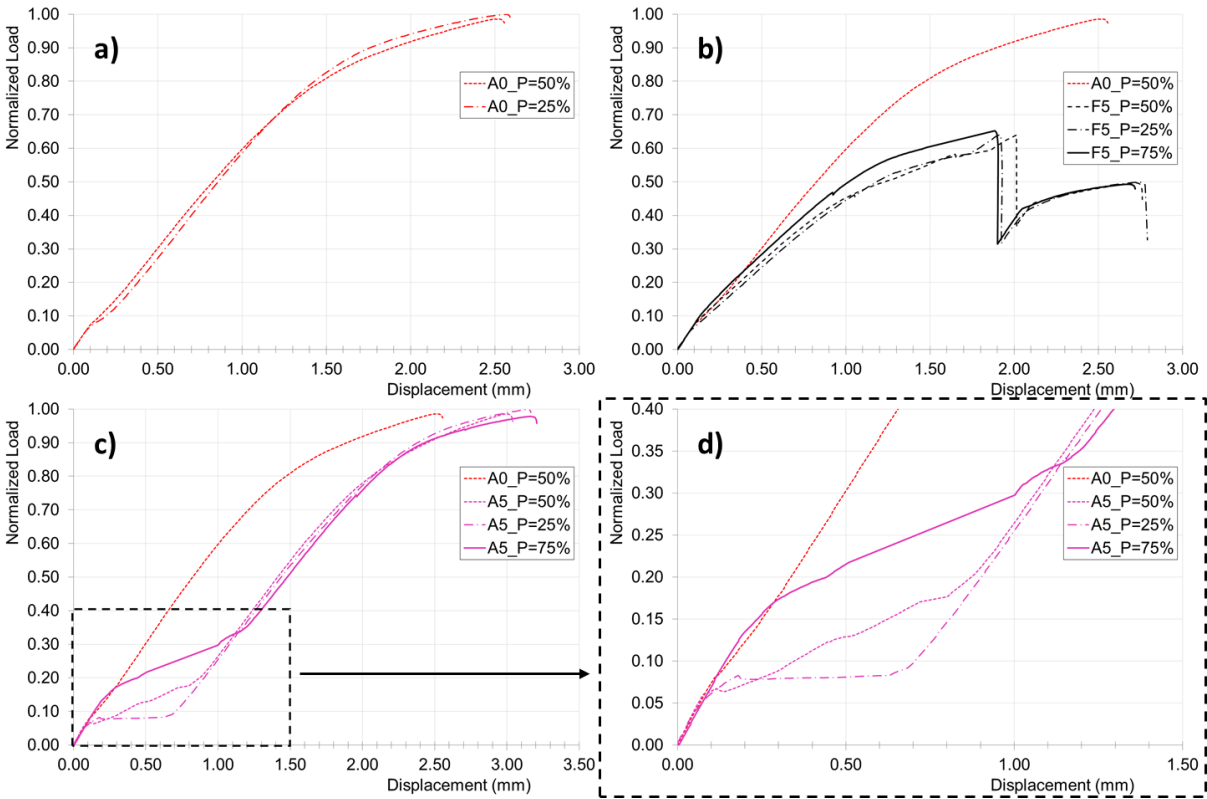

Figure 20 : Effect of preload on static behavior: a) configuration *A0*, b) configuration *F5*, c) configuration *A5*, and d) zoom on sliding phase *A5*
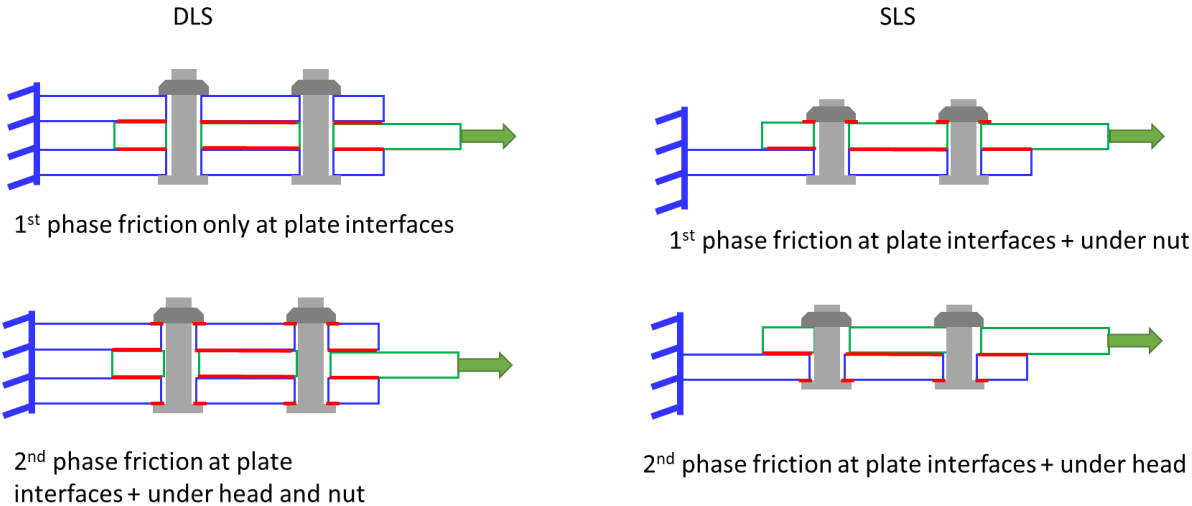

Figure 21 : Difference of slipping behavior between SLS and DLS specimen

4.3.2. Fatigue impact of bolt preload

The S-N curves of a hole-to-hole bolted assembly under different tightening levels for configurations *A5* and *F5,* representative of clearance and misalignments respectively, are shown in Figure 22 and Figure 23. In both configurations, increasing the preload leads to an increase in the fatigue life of the joints as expected. The KFI, extracted from S-N curves, are plotted against bolt preload level in Figure 24. For joints with bolt hole clearance, increasing bolt preload level from 25% to 50% leads to an 18% increase in the KFI. However, increasing the bolt preload from 50% to 75% leads to a similar fatigue strength, as if a threshold had been reached. Configuration *F5* shows different behavior. Increasing bolt preload from 25% to 50% leads to a lower increase in the KFI, of around 7%. However, increasing bolt preload from 50% to 75% leads to a similar KFI increase. In both cases these tests show that increasing the bolt preload gives the joint a fatigue life that is longer than that of a reference assembly without bolt hole clearance or hole misalignments (*A0*).

The fatigue failure locations and profiles for several preload levels are shown in Figure 25. Regarding failure locations, previous observations are confirmed as similar results can be observed and representative failures are located at the same hole for configurations *A5* and *F5*: on the nut side. It can be observed that *A5* and *F5* present the same failure location whatever the preload level. Previous works from **[21]** have demonstrated that the site of initiations depends strongly on the bolt preload, and these new results are in agreement. At a low preload level, the failure occurs in the net section of the specimens. Then, at a medium preload level, the failure is shifted slightly towards the edge of the hole and the fastener shank remains visible on failure profiles. At a high preload level, the failure is fully outside the hole and the fastener shank is not visible when the failure profile is observed.

The conclusions that can be drawn from this test case are the following:

- Bolt preload has no impact on the ultimate static strength of joints. The hypotheses to explain this phenomenon is that when the bolt shearing occurs the clamping load is strongly decreased. As the clamping load is decreased the friction load is also decreased so the remaining transfer bolt is only carried by the bolts up to their limit in shear independent of the preload level. This statement can, be verified by the use of finite element models.

- Increasing bolt preload delays the macro-slipping to a higher slipping load. This conclusions is consistent with the literature. Increasing the clamping load increases the frictional load at the interface, simple demonstration trough Coulomb's law. Thus the slipping occurs at a higher load level.

- Fatigue strength increases when bolt preload is increased up to a certain limit. This limit appears to be further for joints hole misalignments. This phenomena is explained by **Benhaddou et al. [21]** trough finite element modelling. Higher preload levels significantly reduce the magnitude of longitudinal tensile stresses in stress concentration areas, thus decreasing the severity of stress concentration and redistributing the stresses in a more effective manner. Misalignment further disrupts the distribution of effort. The effort required for redistribution therefore appears to be greater.

- The fatigue failure location depends on bolt preload for joints with or without clearance and misalignments. There is two level of observations first the side of the failure (green part or blue parts i.e. head side or nut side), second the location around the hole (net section / slightly shifted / fully shifted) The side of the failure is mainly influenced by the H2H configuration. While the location around the hole is mainly linked to the bolt technology and the bolt preload level."
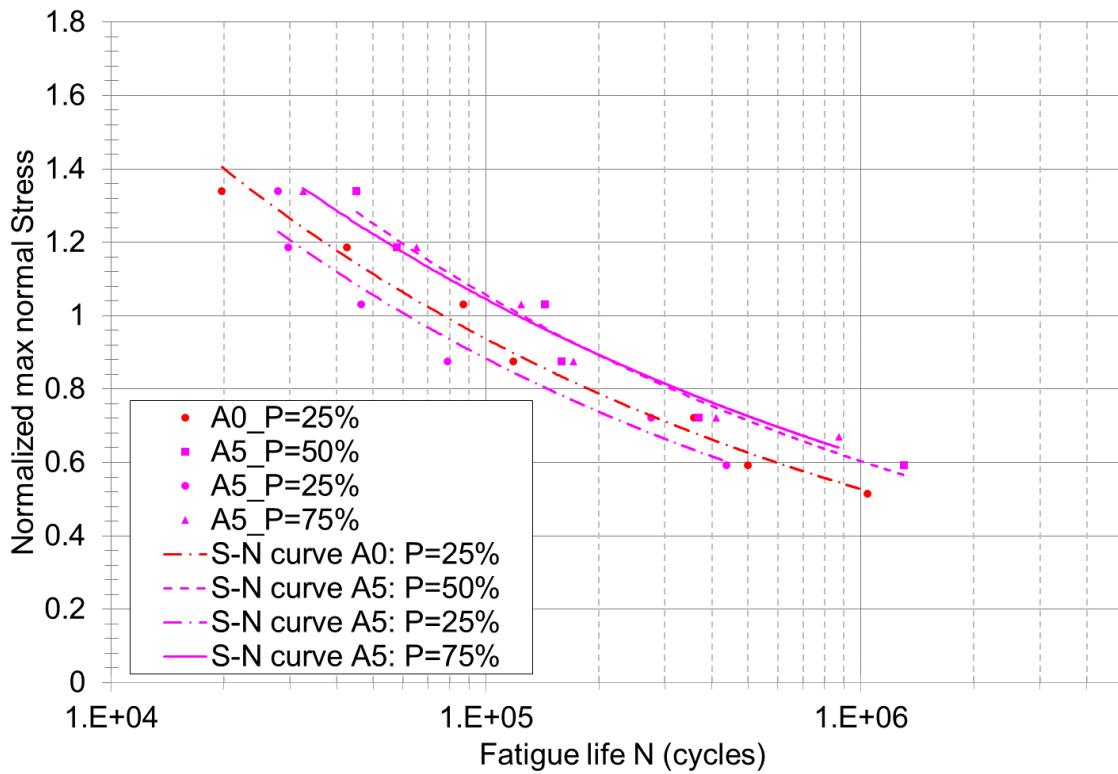
Figure 22 : Fatigue life for bolted joints with clearance at different preload levels
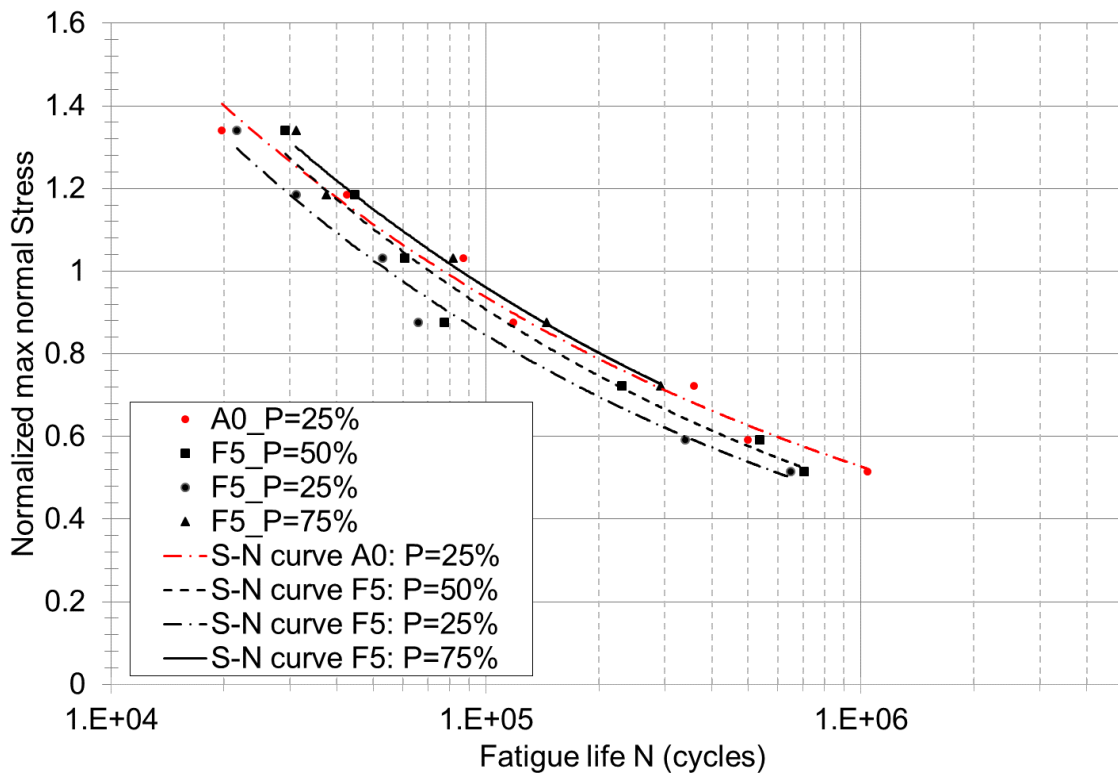

Figure 23 : Fatigue life for bolted joints with clearance and misalignments at different preload levels
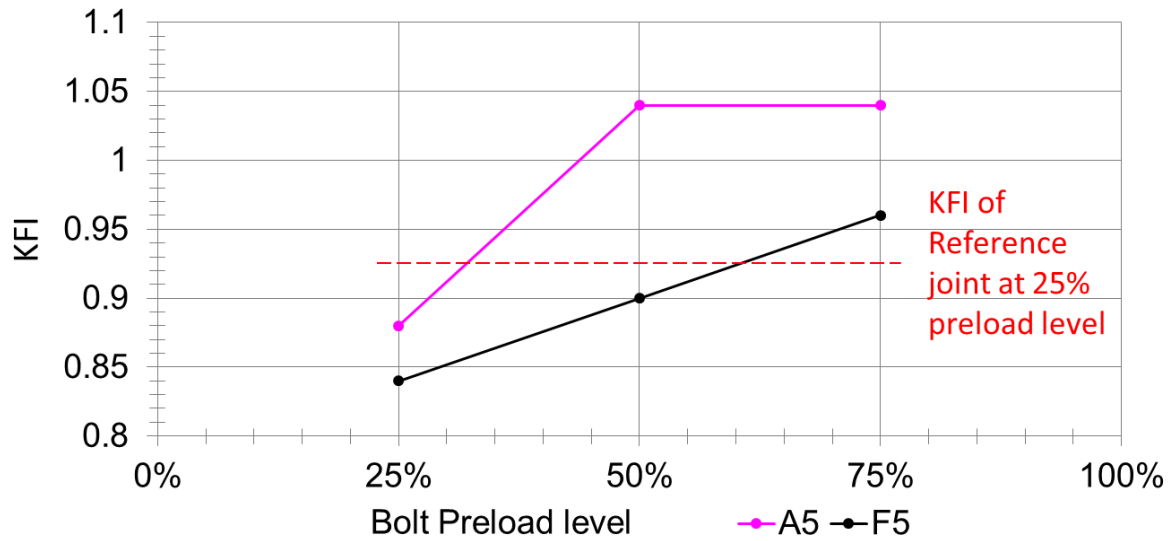
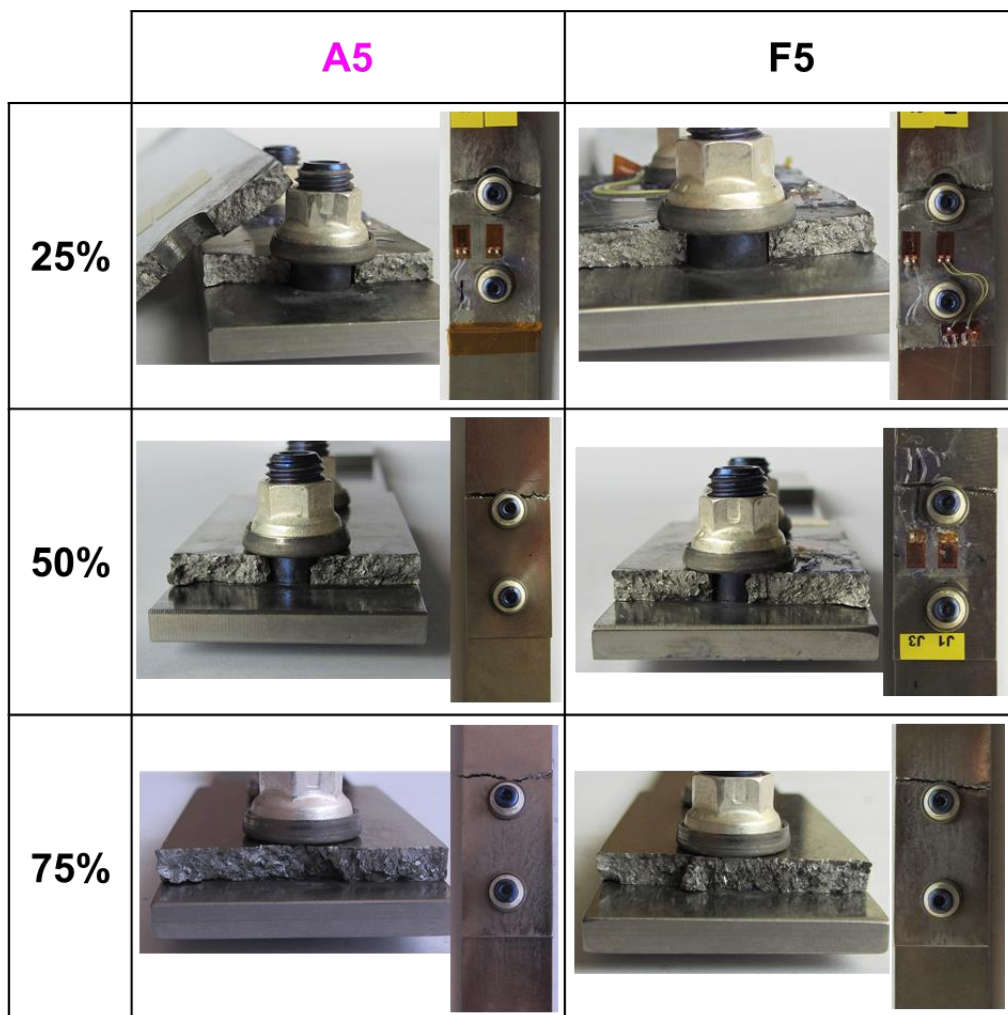**Figure 24 : KFI for bolted joints with clearance and misalignments at different preload levels**

Figure 25 : Fatigue failure locations for configurations A5 and F5 at different preload levels

5. Conclusions

The effects of clearance and misalignments in two-bolt, single-lap, titanium joints on quasi-static strength, fatigue life and failure modes have been studied experimentally. To the authors' knowledge this is the first time that the effects of misalignment are investigated experimentally. The impact of defects induced by H2H was evaluated for different assembly parameters such as bolt preload, bolt diameter and thickness of plates.

Overall, the results indicate that opposite misalignments constitute the worst case scenario as they result in lower quasi static strength, with a 36% decrease in the ultimate load, and a 14% decrease in the Key Fatigue Indicator, relative to a reference joint.

The observation of failure modes showed a strong difference of load distributions in the fasteners, which explained such knock down of static and fatigue strength.

However, investigations on assembly parameters provided potential solutions to decrease the performance gap between perfect-fit joints and H2H joints. Increasing bolt diameter or decreasing plate thickness lessens the decrease of static strength induced by misalignments. Increasing bolt preload improves the fatigue life of bolted joints despite clearance and misalignments.

To complete this work, further analysis are under progress. Especially ones using Finite Element Method to demonstrate the observed behaviour and provide design rules to guide the manufacturing specifications of aeronautical joints with high load transfers.

References

[1] P. Fontanet-Pérez, X H. Vázquez, D. Carou, The impact of the COVID-19 crisis on the US airline market: Are current business models equipped for upcoming changes in the air transport sector?, Case Studies on Transport Policy, 10, 2022, pp.647-656, https://doi.org/10.1016/j.cstp.2022.01.025.

[2] J. Hoelzen, D. Silberhorn, T. Zill, B. Bensmann, R. Hanke-Rauschenbach, Hydrogen-powered aviation and its reliance on green hydrogen infrastructure – Review and research gaps, International Journal of Hydrogen Energy, 47(5), 2022, pp.3108-3130, https://doi.org/10.1016/j.ijhydene.2021.10.239.

[3] J E. Muelaner*, O C. Martin, P G. Maropoulos, Achieving Low Cost and High Quality Aero Structure Assembly through Integrated Digital Metrology Systems. Procedia CIRP, 7, 2013, pp 688-693, https://doi.org/10.1016/j.procir.2013.06.054.

[4] J. Bloem Developments in Hole-to-Hole Assembly. SAE Transactions, 116, 2007, pp.1087-1097, http://www.jstor.org/stable/44719545

[5] S.K. Bhaumik, M. Sujata, M.A. Venkataswamy, Fatigue failure of aircraft components, Engineering Failure Analysis, Volume 15, Issue 6, 2008, Pages 675-694, https://doi.org/10.1016/j.engfailanal.2007.10.001.

[6] J. Andriamampianina, F. Alkatan, P. Stéphan, J. Guillot, Determining load distribution between the different rows of fasteners of a hybrid load transfer bolted joint assembly, Aerospace Science and Technology, 23 , 2012, pp.312-320. https://doi.org/10.1016/j.ast.2011.08.008.

[7] X. Yuan, Z.F. Yue, W.Z. Yan, S.F. Wen, L. Li, Experimental and analytical investigation of fatigue and fracture behaviors for scarfed lap riveted joints with different lap angle, Engineering Failure Analysis, 33, 2013, pp 505-516, https://doi.org/10.1016/j.engfailanal.2013.05.019.

[8] F. Shen, Y. Zhang, Continuum damage mechanics based approach to study the effects of the scarf angle, surface friction and clamping force over the fatigue life of scarf bolted joints, International Journal of Fatigue, 102, 2017, pp 59-78, https://doi.org/10.1016/j.ijfatigue.2017.04.008.

[9] J. Lecomte, C. Bois, H. Wargnier, J-C. Wahl, An analytical model for the prediction of load distribution in multi-bolt composite joints including hole-location errors, Composite structures, 117, 2014, pp.354-361, https://doi.org/10.1016/j.compstruct.2014.06.040.

[10] F. Liu, M. Shan, L. Zhao, J. Zhang, Probabilistic bolt load distribution analysis of composite single-lap multi-bolt joints considering random bolt-hole clearances and tightening torques, Composite Structures, 194, 2016, pp.12-20, https://doi.org/10.1016/j.compstruct.2018.03.100.

[11] R. Askri, C. Bois, H. Wargnier, Effect of Hole-location Error on the Strength of Fastened Multi-Material Joints, Procedia CIRP, 43, 2018, pp.292-296, https://doi.org/10.1016/j.procir.2016.02.040

[12] R Askri, C. Bois, H. Wargnier, N. Gayton, Tolerance synthesis of fastened metal-composite joints based on probabilistic and worst-case approaches, Computer-Aided Design, 100, 2018, pp.39-51, https://doi.org/10.1016/j.cad.2018.02.008.

[13] M.A McCarthy, V.P. Lawlor, W.F. Stanley, C.T. McCarthy, Bolt-hole clearance effects and strength criteria in single-bolt, single-lap, composite bolted joints, Composites Science and Technology, 62 (10–11,) 2002, pp.1415-1431, https://doi.org/10.1016/S0266-3538(02)00088-X

[14] Y. Cao, Z. Cao, Y. Zuo, L. Huo, J. Qiu, D. Zuo, Numerical and experimental investigation of fitting tolerance effects on damage and failure of CFRP/Ti double-lap single-bolt joints, Aerospace Science and Technology, 78, 2018, pp 461-470, https://doi.org/10.1016/j.ast.2018.04.042.

[15] C. Liu, Y. Li, Y. Cheng, X. Li, S. Cao, H. Cheng, B. Luo, Investigation on deformation of composite multi-bolted joints considering influences of hole-location errors and installation sequence, Engineering Failure Analysis, Volume 140, 2022, https://doi.org/10.1016/j.engfailanal.2022.106592.

[16] A. Gupta, C. J. Bennett, W. Sun, Fatigue property-performance relationship of additively manufactured Ti-6Al-4V bracket for aero-engine application: An experimental study, Procedia Structural Integrity, Volume 38, 2022, pp.40-49, https://doi.org/10.1016/j.prostr.2022.03.005.

[17] T.N. Chakherlou, M. Mirzajanzadeh, J. Vogwell, B. Abazadeh, Investigation of the fatigue life and crack growth in torque tightened bolted joints, Aerospace Science and Technology, Volume 15, 2011, pp 304-313, https://doi.org/10.1016/j.ast.2010.08.003.

[18] T.N. Chakherlou, H. Taghizadeh, A.B. Aghdam, Experimental and numerical comparison of cold expansion and interference fit methods in improving fatigue life of holed plate in double shear lap joints, Aerospace Science and Technology, Volume 29, 2013, pp 351-362, https://doi.org/10.1016/j.ast.2013.04.006.

[19] J. Hu, K. Zhang, H. Cheng, Z. Qi, An experimental investigation on interfacial behavior and preload response of composite bolted interference-fit joints under assembly and thermal conditions, Aerospace Science and Technology, Volume 103, 2020, 105917, https://doi.org/10.1016/j.ast.2020.105917.

[20] T. Dang Hoang, C. Herbelot, A. Imad, On failure mode analysis in a bolted single lap joint under tension-shearing, Engineering Failure Analysis, Volume 24, 2012, Pages 9-25, https://doi.org/10.1016/j.engfailanal.2012.03.006.

[21] T. Benhaddou, P. Stephan, A. Daidié, F. Alkatan, C. Chirol, JB. Tuery, Effect of axial preload on durability of aerospace fastened joints, International Journal of Mechanical Sciences, 137, 2018, pp.214-223, https://doi.org/10.1016/j.ijmecsci.2018.01.023

[22] J.F. Ramière,. C. Briançon, F. Chéret, J.P. Jeandrau, M. Leroy, J. Renard, A. Thionnet, Jonctions hybrides boulonnées-collées. Application aux cas des structures d'avions. Revue des Composites et des Matériaux Avancés, 20(2), 2010, pp 215-232, https://doi:10.3166/rcma.20.215-232

[23] J. Guillot, Calcul des assemblages vissés. Assemblages de pièces planes de faibles épaisseurs. Partie 1, Tech de l'ingénieur BM 5564, 2010, pp.1-20, https://doi.org/10.51257/a-v1-bm5564

[24] J. Guillot, Calcul des assemblages vissés. Assemblages de pièces planes de faibles épaisseurs. Partie 2, Tech de l'ingénieur BM 5563, 2011, pp 1-16,

[25] X. Liu, X. Xi, C. Bai, J. Yang, X. Yang, Dynamic response and failure mechanism of Ti-6AL-4V hi-lock bolts under combined tensile-shear loading, International Journal of Impact Engineering, Volume 131, 2019, pp 140-151, https://doi.org/10.1016/j.ijimpeng.2019.04.025.

[26] J. Huet, Du calcul des assemblages par boulons ou rivets travaillant en cisaillement, Publication du CETIM : les assemblages mécaniques : tendances actuelles et perspectives. (isbn 2-85400-328-4), 25-26, 1995, pp 133 -147

[27] M. Rodrigues, J. Correia, B. Pedrosa, A. Jesus, B. Carvalho, C. Rebelo, J. Xavier, R. Calçada, Numerical Analysis of a Double Shear Standard Bolted Connection Considering Monotonic Loadings. Engineering Structures and Technologies, 2017, pp 183-194, : https://doi.org/10.3846/2029882X.2017.1414638